

BIG BANG NUCLEOSYNTHESIS: THEORIES AND OBSERVATIONS

Ann Merchant Boesgaard

Institute for Astronomy, University of Hawaii, Honolulu, Hawaii 96822

Gary Steigman

Bartol Research Foundation, University of Delaware, Newark, Delaware
19716

1. INTRODUCTION

Other than the blackbody spectrum of the microwave background, there is very little direct evidence in support of the nearly universally accepted hot Big Bang model of cosmology—the “standard” model. Primordial nucleosynthesis provides a unique opportunity to test the assumptions of the standard model, serving, as it does, as a probe of the physical conditions during epochs in the early evolution of the Universe that would otherwise be completely hidden from our scrutiny. In contrast with much that is currently very exciting in modern physical cosmology, the predictions of Big Bang nucleosynthesis may be directly confronted with observational data. The primordial abundances of the light elements synthesized during the first few minutes in the evolution of the Universe described by the standard model may be compared with the pregalactic abundances of the elements inferred from observational data. The early qualitative successes in such comparisons of the standard model have, in recent years, led to much more detailed quantitative comparisons. In this review we summarize the predictions of the standard model, evaluate critically the implications of

the current observational data, and provide a report card on the hot Big Bang model.

It is not our intent here to review the history of the study of Big Bang nucleosynthesis. Weinberg (1977), in his excellent little book, *The First Three Minutes*, provides a lucid account of this fascinating tale. Schramm & Wagoner (1977) summarize briefly some of the early work in their review. Truran (1984) includes a section on element synthesis in the Big Bang in his review of nucleosynthesis. Pagel (1982) reviews the relevant observational data. To provide our readers with a self-contained description of the evaluation of the Universe during the element building epochs, we begin with an overview of the standard hot Big Bang model, concentrating on the physics of importance to primordial nucleosynthesis. We describe the synthesis of the elements in the standard model and present the quantitative predictions of the abundances. Next, we consider the consequences of varying the assumptions of the standard model. Then we turn to the data, where we review the most relevant observations and attempt to infer from them the primordial abundances (or limits to them). Our best estimates—from the data—of the primordial abundances are compared with the theoretical predictions of the standard model, as well as with those of models that deviate from the standard one. We check for consistency of the standard model and derive bounds to the nucleon density, the number of light neutrino species, anisotropy, neutrino degeneracy, etc. The cosmological consequences of our critical comparison of theory and observation are discussed. In our concluding remarks we comment on those aspects of theory and observation that need further work.

2. THE STANDARD HOT BIG BANG MODEL

On the largest scales the present Universe is observed to be homogeneous and is expanding isotropically. If the isotropy and homogeneity were exact, the space-time would be described by a unique metric, the Robertson-Walker metric, which involves a time-dependent scale factor $a(t)$ and a dimensionless constant k measuring the three-space curvature. The evolutionary history of the cosmological model describing our Universe is contained in the time dependence of the scale factor. If the Robertson-Walker metric is used in the Einstein equations, the Friedmann models emerge. For the Robertson-Walker-Friedmann models, the evolution of the scale factor is described by the solutions to

$$H^2 = \left[\frac{1}{a} \left(\frac{da}{dt} \right) \right]^2 = \frac{8\pi}{3} G\rho - \frac{kc^2}{a^2} + \frac{\Lambda}{3}. \quad 1.$$

In Equation 1, $H = H(t)$ is the Hubble parameter, $\rho = \rho(t)$ is the total mass density, and Λ is the cosmological constant (G is Newton's constant and c is the speed of light). For nonrelativistic (NR) matter, the mass density is proportional to the particle number density ($\rho_{\text{NR}} = mn$), which (for conserved particles) varies as $n \propto a^{-3}$. In contrast, the mass (energy) density of relativistic (R) particles (radiation) is proportional to the number density *times* the average energy per particle. Now, all momenta p are inversely proportional to wavelengths λ (de Broglie wavelength), and all wavelengths vary according to the scale factor ($p \propto \lambda^{-1} \propto a^{-1}$), so that $\rho_{\text{R}} \propto a^{-4}$.

Equation 1 may be written in terms of the present values (indicated by the subscript zero) of various quantities:

$$\left(\frac{H}{H_0}\right)^2 = \Omega_{\text{R}}\left(\frac{a_0}{a}\right)^4 + \Omega_{\text{NR}}\left(\frac{a_0}{a}\right)^3 + \frac{kc^2}{H_0^2 a_0^2} \left(\frac{a_0}{a}\right)^2 + \frac{\Lambda}{3H_0^2}. \quad 1'$$

In Equation 1' we have introduced $\Omega \equiv \rho/\rho_{\text{c}}$, where the "critical" (or Einstein-de Sitter) density is $\rho_{\text{c}} \equiv 3H_0^2/8\pi G$.

The *early* ($t \ll t_0$) evolution of the Universe is "radiation dominated" (RD), since (for $a \ll a_0$)

$$H^2 \approx \frac{8\pi}{3} G\rho_{\text{R}}. \quad 2.$$

Integrating Equation 2, we obtain

$$\frac{32\pi}{3} G\rho_{\text{R}} t^2 = 1. \quad 3.$$

Since, for radiation, the energy density varies as the fourth power of the temperature T , it follows from Equation 3 that $T \propto t^{-1/2}$; as time goes on, the Universe expands and cools. To a good approximation, when the Universe is ~ 1 s old, the radiation temperature is $\sim 10^{10}$ K, or $kT \approx 1$ MeV.

2.1 The Epoch of Nucleosynthesis

Since we are concerned with nuclear reactions, the relevant energy scale is measured in MeV and the appropriate length scales are in fermis ($1 \text{ f} = 10^{-13} \text{ cm}$). During the epoch of interest the Universe consists of a *dilute* gas of photons (γ), neutrinos (ν), electron-positron pairs (e^\pm), and trace amounts of nucleons (N). For example, if the temperature is measured in energy units (MeV), the number density of blackbody photons is $n_\gamma = 10^{-7.5} T_{\text{MeV}}^3 \text{ f}^{-3}$. Therefore, on average, the length scale associated with this

number density is

$$l_\gamma \equiv n_\gamma^{-1/3} \approx 300 T_{\text{MeV}}^{-1} \text{ f.} \quad 4.$$

This length greatly exceeds the nuclear scale. At high temperatures, when they are extremely relativistic, the densities of e^\pm 's and ν 's are comparable to those of γ 's, so that $l_e \approx l_\nu \approx l_\gamma$. During the epochs of interest ($10 > T_{\text{MeV}} > 10^{-2}$), nucleons are a trace contaminant: $n_N \equiv \eta n_\gamma$, where $\eta < 10^{-9}$, so that $l_N > 10^3 l_\gamma$.

Although particles are far apart, reactions are occurring rapidly. For a "typical" cross section of $\sim 1 \text{ f}^2$ (most relevant collisions have much larger cross sections), each particle suffers very many collisions in one expansion time: $ct \approx (10^{16} T_{\text{MeV}}) l_{\text{coll}}$, where l_{coll} is the distance between collisions. As a result, equilibrium is established and maintained very rapidly; deviations from equilibrium are quickly erased.

Finally, we note that the size of the "causal" horizon is very large: $l_H \approx ct \approx 10^{23.5} T_{\text{MeV}}^{-2} \text{ f}$; $l_\gamma/l_H \approx 10^{-21} T_{\text{MeV}}$, $l_{\text{coll}}/l_H \approx 10^{-16} T_{\text{MeV}}^{-1}$. However, at these early epochs ($10^{-2} < t < 10^3 \text{ s}$), the mass of nucleons within the horizon is very small: $M_N \approx 10^{-3} T_{\text{MeV}}^{-3} M_\odot$.

Since details of the earlier history are erased, the only free parameter needed to characterize the epoch of nucleosynthesis is $\eta = n_N/n_\gamma$, the ratio of nucleons to photons. We begin our description of Big Bang nucleosynthesis when the Universe is $\sim 10 \text{ ms}$ old.

2.1.1 $t > 10^{-2} \text{ s}$ ($T < 10^{11} \text{ K}$) At such early times collisions are so rapid that even the weak interactions are in equilibrium. Through the *neutral current* weak interaction, *all* light neutrino species ($m_\nu < T$) are kept in equilibrium with e^\pm 's via $e^+ + e^- \leftrightarrow \nu_i + \bar{\nu}_i$ ($i = e, \mu, \tau, \dots$). In equilibrium, the number and mass densities of neutrinos, compared to those of photons are

$$\frac{n_\nu}{n_\gamma} = \frac{3}{4} N_\nu, \quad N_\nu = \sum_i \frac{1}{2} g_{\nu i}, \quad 5a.$$

$$\frac{\rho_\nu}{\rho_\gamma} = \frac{7}{8} N_\nu. \quad 5b.$$

In Equation 5, N_ν is the number of light two-component neutrinos, and $g_{\nu i}$ is the number of helicity states of neutrino type i .

The neutron-to-proton ratio is maintained at its equilibrium value,

$$n/p = \exp(-\Delta m/T), \quad 6.$$

by the *charged current* weak interactions: $p + e^- \leftrightarrow n + \nu_e$, $n + e^+ \leftrightarrow p + \bar{\nu}_e$; occasionally, beta decay (also inverse decay) $n \rightarrow p + e^- + \bar{\nu}_e$ occurs.

2.1.2 $t \approx 0.1 \text{ s}$ ($T \sim 3 \times 10^{10} \text{ K}$) When the temperature drops to a few MeV, the neutral current weak interactions become too slow to keep up with the expansion rate and the neutrinos “decouple.” That is, for $T < \text{few MeV}$, virtually no “new” neutrino pairs are produced and no “old” pairs annihilate; the relic neutrinos freely expand with the Universe, their momenta *decreasing* in proportion to the growth of the scale factor: $n_\nu \propto T_\nu^3 \propto a^{-3}$. [All neutrinos (e , μ , τ , . . .) have neutral current weak interactions with e^\pm . Since e -neutrinos *also* have charged current interactions, they decouple somewhat later at a slightly lower temperature.] At this epoch, the charged current weak interactions (“beta decay”) are still occurring sufficiently rapidly to maintain the neutron-to-proton ratio at its equilibrium value (Equation 6).

2.1.3 $t \approx 1 \text{ s}$ ($T \approx 10^{10} \text{ K}$) For $T = T_* \approx 1 \text{ MeV}$, the charged-current weak interactions become too slow to maintain neutron-proton equilibrium. Since the neutron is heavier than the proton, reactions converting neutrons to protons *still occur* but not at a rate sufficient to maintain the ratio at its equilibrium value. At T_* , the neutron-to-proton ratio effectively “freezes out.” To a first approximation, for $T < T_*$,

$$\frac{n}{p} \approx \left(\frac{n}{p} \right)_* = \exp \left(\frac{-\Delta m}{T_*} \right). \quad 7.$$

The freeze-out temperature T_* is determined by the competition between the weak interaction rate $\Gamma = nv\sigma_{wk}$ and the expansion rate $H \sim t^{-1}$. Roughly speaking, the number of reactions (per particle) occurring in one expansion time is $\sim \Gamma t$. Since $n \propto T^3$, $\sigma_{wk} \propto T^2$ (for $T < M_w$, where M_w is the mass of the W-boson), and $t \propto T^{-2}$ as the Universe expands and cools, we have $\Gamma(T)t(T) \propto T^3$. For $T = T_*$, $\Gamma(T_*)t(T_*) \approx 1$. Now the rate Γ is “normalized” by the strength of the charged-current interactions, which is measured by the half-life for neutron beta decay: $\Gamma \propto \tau_n^{-1}$. On the other hand; it is the total energy density of relativistic particles ($m < T$) that determines the universal expansion rate (see Equation 3). At this epoch, γ ’s, ν ’s, and e^\pm ’s are all relativistic, so that

$$\rho_R = \rho_\gamma + \rho_\nu + \rho_e = (g_{\text{eff}}/2)\rho_\gamma, \quad 8a.$$

$$g_{\text{eff}} = \frac{43}{4} \left[1 + \frac{7}{43} (N_\nu - 3) \right]. \quad 8b.$$

In Equation 8, g_{eff} is the “effective” number of relativistic degrees of freedom (helicity states); we have counted two polarizations for γ , four helicity states for e^\pm , and two for each light neutrino species. For example, should the τ -neutrino be “heavy” ($m_{\nu_\tau} \gg 1 \text{ MeV}$), then $N_\nu = 2$ and $g_{\text{eff}} = 9$. In contrast, if

there is a fourth family of leptons with a light neutrino, then $N_\nu = 4$ and $g_{\text{eff}} = 12.5$. Substituting Equation 8 into Equation 3, we find

$$t \text{ (s)} = 2.4 g_{\text{eff}}^{-1/2} T_{\text{MeV}}^{-2}. \quad 9.$$

The more species of relativistic particles, the larger g_{eff} and the faster the Universe expands.

To return to T_* , the neutron/proton “freeze-out” temperature, we note that T_* depends on the competition between the weak interaction rate ($\Gamma \propto \tau_n^{-1}$) and the expansion rate ($t^{-1} \propto g_{\text{eff}}^{-1/2}$): $T_* \propto (g_{\text{eff}}^{1/2} \tau_n)^{1/3}$. If the precise value of the neutron half-life were known, the neutron abundance $(n/p)_*$ would be a sensitive probe of the early expansion rate and, hence, of the number of relativistic degrees of freedom $g_{\text{eff}}(T_*)$. We return to this connection later.

2.1.4 $t \approx 10 \text{ s}$ ($T \approx 3 \times 10^9 \text{ K}$) For high temperatures, e^\pm 's and γ 's are maintained in equilibrium by pair production and annihilation ($e^+ + e^- \leftrightarrow \gamma + \gamma$) and Compton scattering ($e^\pm + \gamma \leftrightarrow e^\pm + \gamma$). When the temperature (in energy units) drops below the electron mass, annihilation continues but pair production effectively ceases, since only those rare photons in the exponential tail of the Bose-Einstein distribution have sufficient energy to produce an e^\pm pair. The annihilations of the e^\pm 's heat the photon gas; more photons (or more precisely, more photon entropy) are produced. Recall that the neutrinos have already decoupled, so that after e^\pm annihilation, we have $T_\gamma > T_\nu$. The ratio of the ν - and γ -temperatures may be calculated by a simple application of entropy conservation (see, for example, Steigman 1979):

$$T_\gamma/T_\nu = (11/4)^{1/3}. \quad 10.$$

After e^\pm annihilation there are more relic photons for each relic neutrino than before. As a consequence, the present ratio of “microwave” neutrinos to microwave photons is

$$\eta_\nu = \left(\frac{n_\nu}{n_\gamma} \right) = \frac{3}{4} \left(\frac{T_\nu}{T_\gamma} \right)^3 N_\nu = \frac{3}{11} N_\nu. \quad 11.$$

If $T_{\gamma 0} = 2.7 \text{ K}$, there are ~ 399 microwave photons and $\sim 109 N_\nu$ relic neutrinos in every cubic centimeter averaged over the Universe.

The reader may wonder why, in our discussion of primordial *nucleosynthesis*, we have yet to consider any *nuclear* reactions. Of course, while all the above weak and electromagnetic interactions were proceeding, the occasional nuclear reaction among neutrons and protons ($n + p \leftrightarrow D + \gamma$) had occurred. However, the deuteron is only very weakly bound and has a large photodissociation cross section. Since the nucleons are merely a trace

contaminant in a bath of radiation ($n_{\text{N}}/n_{\gamma} = \eta < 10^{-9}$), as soon as the deuteron is formed, it is immediately photodissociated. The rapid photodissociation of the deuteron keeps the deuterium abundance very small (see Figure 1 and discussion in the following section) and imposes a bottleneck to any further nucleosynthesis. Thus far, roughly 10 s into the evolution of the Universe, no significant nucleosynthesis has yet occurred (see Figure 1).

2.1.5 $t > 10^2$ s ($T < 10^9$ K) As the Universe expands and cools, fewer and fewer photons are capable of photodissociating the deuteron. The number of such photons per nucleon varies as $\eta^{-1} \exp(-2.2/T_{\text{MeV}})$, so that for $T < T_{\text{D}\gamma} \approx 0.1$ MeV, the deuterium abundance increases. Since $T_{\text{D}\gamma}^{-1} \approx a - b \ln \eta$, the higher the nucleon abundance η , the higher the temperature

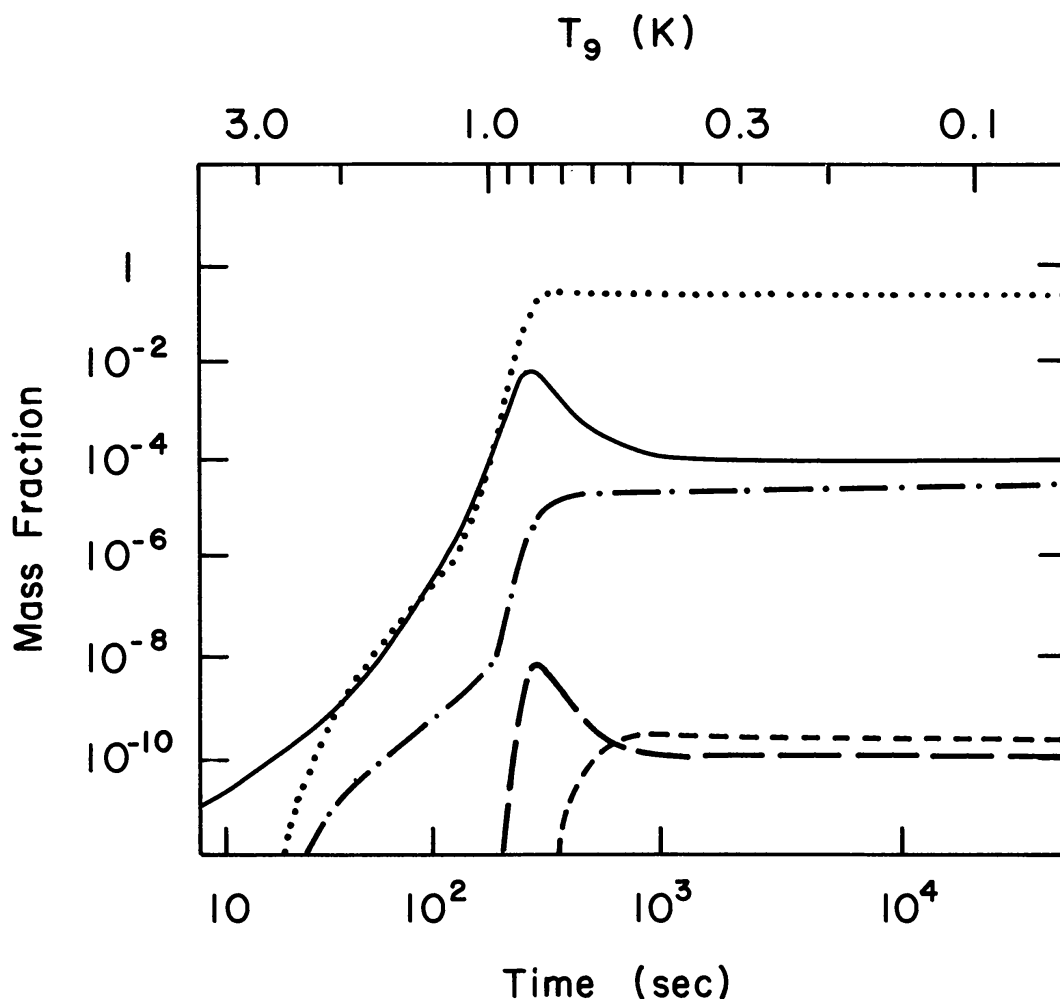


Figure 1 The evolution of nuclear abundances in the standard hot Big Bang model. The dotted line is for ${}^4\text{He}$, the solid line is D , the dashed-dotted line is ${}^3\text{He}$, the long-dashed line is ${}^7\text{Li}$, and the short-dashed line is ${}^7\text{Be}$, which electron captures to form ${}^7\text{Li}$. (After Wagoner 1973.)

$T_{D\gamma}$ at which the deuterium bottleneck is overcome—the earlier nucleosynthesis begins in earnest. With the deuterium abundance increasing, there is finally a platform to stand on to build up the heavier elements. Tritium is formed by $d(n, \gamma)^3\text{H}$ and $d(d, p)^3\text{H}$ reactions and ^3He via $d(p, \gamma)^3\text{He}$ and $d(d, n)^3\text{He}$; ^3H and ^3He interconvert by $^3\text{He}(n, p)^3\text{H}$ and $^3\text{H} \rightarrow ^3\text{He} + e^- + \bar{\nu}_e$. Tritium is burned to ^4He via $^3\text{H}(p, \gamma)^4\text{He}$ and $^3\text{H}(d, n)^4\text{He}$, while ^4He is synthesized from ^3He by $^3\text{He}(n, \gamma)^4\text{He}$, $^3\text{He}(d, p)^4\text{He}$, and $^3\text{He}(^3\text{He}, 2p)^4\text{He}$. For the rates of these and all other relevant reactions, the reader is referred to Schramm & Wagoner (1977), Fowler et al. (1975), Harris et al. (1983), and Yang et al. (1984, hereafter YTSSO).

The gaps—no stable nuclei—at mass-5 and mass-8 provide bottlenecks to further nucleosynthesis. Even without these gaps, the coulomb barriers, which increase as the Universe cools, prevent the synthesis of significant abundances of the elements heavier than helium (Dicus & Teplitz 1980). Some trace amounts of ^7Li and ^7Be are produced via $^4\text{He}(^3\text{H}, \gamma)^7\text{Li}$ and $^4\text{He}(^3\text{He}, \gamma)^7\text{Be}$.

2.1.6 $t > 10^3 \text{ s } (T < 4 \times 10^8 \text{ K})$ For $T_{\text{MeV}} < 0.03$, the coulomb barriers become so large that nucleosynthesis is effectively terminated (see Figure 1). Because of the gap at mass-5 and the coulomb barriers, most of the neutrons that were present when nucleosynthesis began at $T_{D\gamma}$ are incorporated in ^4He —the most tightly bound light nucleus. Since each alpha particle contains two neutrons, a rough estimate of the primordial ^4He mass fraction Y_p is twice the neutron mass fraction at $T_{D\gamma}$: $Y_p \approx 2X_n(T_{D\gamma})$. Furthermore, in the time between neutron “freeze-out” at T_* and the start of nucleosynthesis at $T_{D\gamma}$, few neutrons have been converted to protons, so that $Y_p \lesssim 2X_n(T_*)$. The primordial abundance of ^4He will, therefore, depend on T_* ; Y_p is most sensitive to the competition between the weak interaction rate and the universal expansion rate. Furthermore, Y_p is insensitive to the nucleon abundance, since for η in the range of interest ($\eta > 10^{-11}$), the two-body reaction rates that build ^4He are sufficiently rapid to incorporate virtually all neutrons in ^4He . In contrast, the primordial abundances of D, ^3He , and ^7Li depend sensitively on η , since they are determined by the competition between two-body reaction rates and the expansion rate. The predicted abundances are shown in Figure 2. (After YTSSO.)

2.2 The Primordial Abundances

The predicted primordial abundances of the light elements as recently calculated by YTSSO in the standard model ($N_\nu = 3$, $\tau_n = 10.6 \text{ min}$) are shown in Figure 2 and Table 1. For D, ^3He , and ^7Li , the abundance, by number, with respect to H (protons) is displayed; the ^4He mass fraction

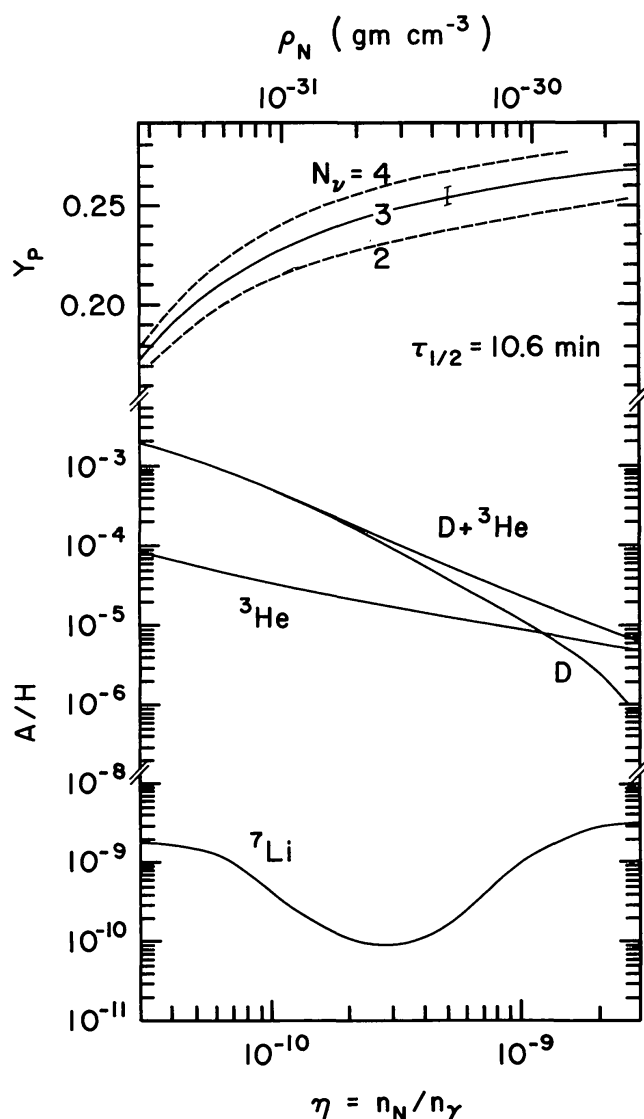


Figure 2 The nuclear abundances predicted by the standard model versus the nucleon-to-photon ratio (lower x-axis) or the nucleon mass density (upper x-axis) (g cm^{-3}) divided by the cube of the temperature in units of 2.7 K. Note the expanded linear scale for Y_p , the primordial ^4He mass fraction; the three curves are for $N_\nu = 2, 3, 4$ neutrino types. The neutron half-life is taken to be 10.6 min; the uncertainty marks correspond to ± 0.2 min. The results for D , ^3He , and ^7Li are plotted as ratios—by number—relative to H . (After YTSSO.)

Y_p is shown for $N_\nu = 2, 3, 4$, and the uncertainty corresponding to $\Delta\tau_n = \pm 0.2$ min is indicated. (Note the very much expanded *linear* scale for Y_p .) On the basis of the discussion above, we may understand the behavior of the abundances as functions of η , N_ν , τ_n , etc.

2.2.1 DEUTERIUM AND HELIUM-3 D and ^3He are burned to ^4He . The larger the nucleon abundance η , the more rapidly are D and ^3He destroyed; hence,

the D and ^3He abundances decrease with increasing η . Since the deuteron is less strongly bound than ^3He and, more importantly, with one unit of charge offers a smaller coulomb barrier, D/H falls more rapidly with increasing η than $^3\text{He}/\text{H}$. It is the competition between two-body reaction rates ($\propto \eta$) and the expansion rate (t^{-1}) that determines the survival of D and ^3He . To a good approximation then, an *increase* in the expansion rate ($t \rightarrow t' = \xi^{-1}t, \xi \geq 1$) is equivalent to a *decrease* in the nucleon abundance: $(\text{D} + ^3\text{He})/\text{H} = f(\eta/\xi)$.

In Figure 2 and Table 1 the sum of the D and ^3He abundances is shown. For $0.2 < 10^{10}\eta < 30$, $(\text{D} + ^3\text{He})/\text{H}$ is well represented by $(5 \times 10^{-4})/\eta_{10}^{1.4}$, where $\eta_{10} \equiv 10^{10}$ (YTSSO).

2.2.2 LITHIUM-7 For relatively low nucleon abundance ($\eta < 3 \times 10^{-10}$), ^7Li is produced mainly by $^4\text{He}(^3\text{H}, \gamma)^7\text{Li}$ and is destroyed by $^7\text{Li}(p, \alpha)^4\text{He}$. As η increases at low η , the abundance of lithium decreases as the ^7Li is burned away. The nonmonotonic behavior of $^7\text{Li}/\text{H}$ as shown in Figure 2 has as its origin an alternate pathway to the synthesis of ^7Li . For $\eta > 3 \times 10^{-10}$, ^7Li is produced by ^7Be -electron capture [$^7\text{Be}(e^-, \nu_e)^7\text{Li}$], the ^7Be having been synthesized via $^4\text{He}(^3\text{He}, \gamma)^7\text{Be}$. The characteristic valley shape shown in Figure 2 is a consequence of these two competing pathways. As a result, for a large range in nucleon abundance ($1/2 < \eta_{10} < 10$), the ^7Li abundance varies by only a small amount: $^7\text{Li}/\text{H} = 0.8\text{--}10 \times 10^{-10}$.

2.2.3 HELIUM-4 As already noted, the gap at mass-5 and the coulomb barriers that grow as the Universe expands and cools conspire to ensure

Table 1 Predicted primordial abundances^a of D, ^3He , ^4He , and ^7Li

$10^{10}\eta$	$10^5(\text{D}/\text{H})$	$10^5(\text{D} + ^3\text{He})/\text{H}$	$10^{10}(^7\text{Li}/\text{H})$	Y_p
1	49	53	4.4	0.225
1.5	25	28	1.8	0.233
2	16	18	1.1	0.237
3	8.1	9.7	0.76	0.243
4	5.1	6.5	1.0	0.246
5	3.6	4.8	1.7	0.248
6	2.7	3.8	2.7	0.250
7.	2.1	3.1	3.9	0.252
8	1.7	2.6	5.3	0.253
9	1.4	2.3	6.9	0.254
10	1.1	2.0	8.6	0.255
15	0.48	1.2	17	0.258
20	0.23	0.87	25	0.261

^aFor $N_\nu = 3$ and $\tau_n = 10.6$ min.

that ${}^4\text{He}$, the most tightly bound light nucleus, will emerge from Big Bang nucleosynthesis as the most abundant nucleus, apart from hydrogen. In Figure 2 the ${}^4\text{He}$ mass fraction Y_p is shown on a very much expanded linear scale. In Table 1 the results are for the “standard” model ($N_\nu = 3$, $\tau_n = 10.6$ min).

In Figure 2 we show the effect of differing numbers of light particles (N_ν); the “error” bar indicates the uncertainty in Y_p , corresponding to a ± 0.2 min uncertainty in the neutron half-life. For a limited—but interesting—range in the nucleon abundance ($1.5 < \eta_{10} < 10$), Y_p is well fit by

$$Y_p = 0.230 + 0.011 \ln \eta_{10} + 0.013(N_\nu - 3) + 0.014(\tau_n - 10.6). \quad 12.$$

For $\Delta N_\nu < 1$ and $\Delta \tau_n < 0.2$, Y_p as evaluated from Equation 12 agrees with the computer calculation to ± 0.001 or better.

Notice that the increase in Y_p with increasing N_ν is a reflection of the speedup in the universal expansion rate when more species of relativistic particles are present: $t \rightarrow t' = \xi^{-1}t$, where

$$\xi = \left(\frac{g_{\text{eff}}}{43/4} \right)^{1/2} = \left[1 + \frac{7}{43} (N'_\nu - 3) \right]^{1/2}, \quad 13a.$$

$$N'_\nu = \sum_{F'} \left(\frac{g_F}{2} \right) \left(\frac{T_F}{T_\nu} \right)^4 + \frac{8}{7} \sum_{B'} \left(\frac{g_B}{2} \right) \left(\frac{T_B}{T_\nu} \right)^4. \quad 13b.$$

In Equation 13, N'_ν is the “effective” number of neutrino species, the primes in the sums indicate that e^\pm and γ are omitted, and F (B) are fermion (boson) species that are relativistic at nucleosynthesis. For the “usual” neutrinos, we have $T_F = T_\nu$ and $\sum_{F'} (g_F/2) = N_\nu$. However, particles that couple more weakly than neutrinos (e.g. gravitons, right-handed neutrinos, etc.) will have “frozen-out” earlier, at a higher temperature, and since they will be colder than the neutrinos ($T_{F,B} \ll T_\nu$), their contribution to N'_ν will be suppressed (Steigman et al. 1979, Olive et al. 1981a). Equivalently, any temperature-independent speedup in the expansion rate ξ will change the predicted primordial abundance of ${}^4\text{He}$: $\Delta Y_p \approx 0.16(\xi - 1)$ for $\xi - 1 \ll 1$.

Since, for the same range in η for which Equation 12 is a good approximation, the sum of the primordial abundances of D and ${}^3\text{He}$ is well represented by $(D + {}^3\text{He})/H = 5 \times 10^{-4}(\xi/\eta_{10})^{1.4}$, there is a direct relation between the predicted mass fraction of ${}^4\text{He}$ and $D + {}^3\text{He}$:

$$Y_p = 0.261 - 0.018 \log [10^5(D + {}^3\text{He})/H] + 0.014(N_\nu - 3) + 0.014(\tau_n - 10.6). \quad 14.$$

The Y_p vs. $(D + {}^3\text{He})/H$ relations are displayed in Figure 3. It is noteworthy that for the standard model, for $1 < 10^5(D + {}^3\text{He})/H < 20$, $0.26 > Y_p > 0.24$.

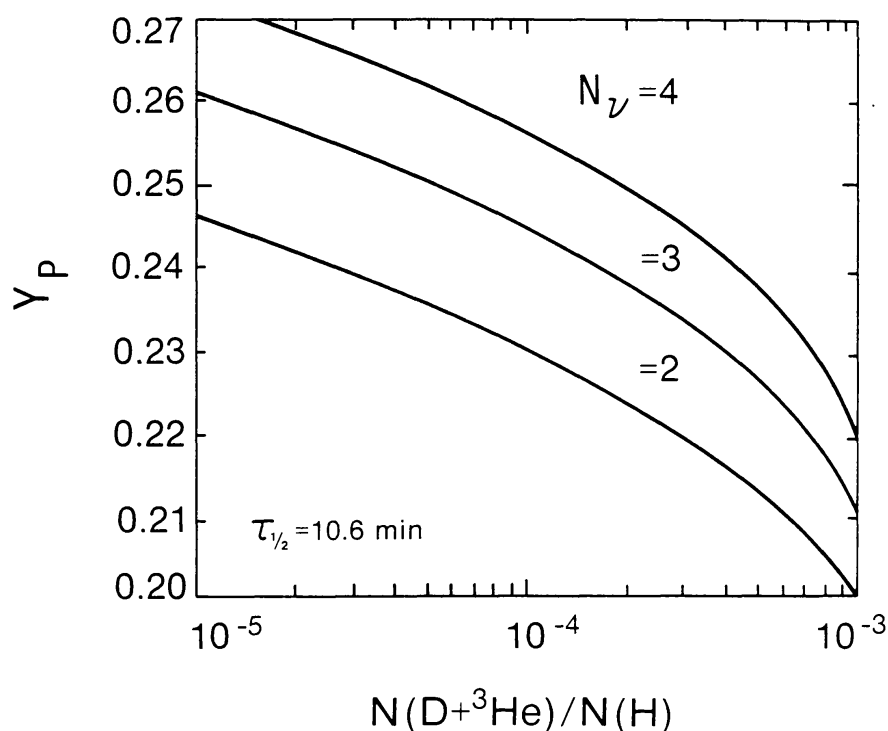


Figure 3 The predicted abundances (by mass) of ${}^4\text{He}$ (Y_p) versus the predicted abundance (by number relative to H) of $\text{D} + {}^3\text{He}$ for $N_\nu = 2, 3, 4$. The neutron half-life is 10.6 min. (From YTSSO.)

2.3 Uncertainties in the Predicted Abundances

The results presented above are from YTSSO, who discussed the sensitivity of the predicted abundances to the uncertainties in the rates of the most relevant reactions. Beaudet & Reeves (1983) have also estimated the residual uncertainties. The calculations of YTSSO employed Wagoner's (1973) reaction rates *with* later revisions by Fowler et al. (1975), G. R. Caughlan & W. A. Fowler (private communication to YTSSO, 1980), and Harris et al. (1983).

If the important reaction rates change by no more than their currently estimated uncertainties, the predicted abundances of D and ${}^3\text{He}$ should be accurate to better than a few percent. For D and ${}^3\text{He}$, then, the accuracy of the predicted abundances far exceeds our ability to estimate the primordial abundances from the observational data. This is *not* the case for ${}^7\text{Li}$. Since ~ 1973 the predicted abundance of ${}^7\text{Li}$ has *increased* by roughly a factor of 3 (Olive et al. 1981b, hereafter OSSTY). The "culprit" has been the reaction ${}^3\text{H}(\text{D}, \text{n}){}^4\text{He}$, whose rate decreased by a factor of order 3 in the relevant temperature range. This decrease in the reaction rate results in an increase in ${}^3\text{H}$, which then may be incorporated in ${}^7\text{Li}$ via ${}^4\text{He}({}^3\text{H}, \gamma){}^7\text{Li}$. A smaller

contribution to the enhanced abundance of ${}^7\text{Li}$ is due to a slight ($\sim 20\%$) reduction in the ${}^7\text{Li}$ destruction rate from ${}^7\text{Li}(\alpha, \gamma){}^{11}\text{B}$. For ${}^7\text{Li}$ there remain uncertainties in several key reaction rates. A factor of ~ 2 uncertainty in the rate of ${}^7\text{Li}$ destruction via ${}^7\text{Li}(p, \alpha){}^4\text{He}$ will, at low nuclear abundance, correspond to a factor of ~ 2 – 3 uncertainty in the predicted abundance. At high nucleon abundance, the yield of ${}^7\text{Be}$ (which will convert to ${}^7\text{Li}$ via electron capture) depends crucially on the rate for ${}^4\text{He}({}^3\text{He}, \gamma){}^7\text{Be}$. Furthermore, the yield of ${}^7\text{Li}$ at high nucleon abundance is sensitive to the rate of ${}^7\text{Be}$ destruction via ${}^7\text{Be}(n, p){}^7\text{Li}$ (Beaudet & Reeves 1983). Given the current uncertainties, the predicted abundance of ${}^7\text{Li}$ is likely to be no more accurate than a factor of 2–3. For ${}^7\text{Li}$, then, the uncertainties in our estimates, from the observational data, of the primordial abundance may be comparable to or even less than the present uncertainties in the predicted abundance.

For a detailed comparison between theory and observation, extremely accurate calculations of the ${}^4\text{He}$ abundance are required. Uncertainties in the nuclear reaction rates introduce less than a 1% uncertainty in the calculated ${}^4\text{He}$ mass fraction. The effects of the weak interaction rates have been considered in greatest detail by Dicus et al. (1982) [see also Cambier et al. (1982) and Johansson et al. (1982)]. Dicus et al. (1982) computed explicitly (rather than fit) the rates of $n \leftrightarrow p$ transitions and correctly treated the Coulomb corrections; they also included finite temperature and finite density radiative corrections, the effect of the plasma on the mass of the electron, and the slight heating of the electron neutrinos (which are almost, but not entirely, decoupled) by e^\pm annihilation. They found a systematic *decrease* of about 1% ($\Delta Y_p \approx -0.003$). This decrease is taken into account in YTSSO and, hence, in Figure 2 and Table 1 here.

There is still a residual uncertainty in Y_p due to the uncertainty in the value of the neutron half-life. Most of the data are consistent with a value in the range $10.4 < \tau_n(\text{min}) < 10.8$ (Christensen et al. 1972, Krohn & Ringo 1975, Stratowa et al. 1978, Erozolimskii et al. 1979, Byrne et al. 1980). Although the low result ($\tau_n = 10.1 \pm 0.1$ min) found by Bondarenko et al. (1978) has generally been ignored, it has recently received some support in the work of Bopp et al. (1984), who derive $\tau_n = 10.3 \pm 0.1$. In contrast, though, Byrne (1984) finds from an analysis of ${}^3\text{H}$ beta decay that $\tau_n = 10.6 \pm 0.1$ min. If it should turn out that τ_n is indeed as small as 10.2 min, the results for Y_p in Figure 2 and Table 1 should be reduced by ~ 0.006 .

In summary, the predicted abundances of D, ${}^3\text{He}$, and ${}^4\text{He}$ should be accurate to a few percent or better; the uncertainty in ${}^7\text{Li}$ may be as large as a factor of 2–3. More precise data on the neutron half-life and on the rates of the reactions ${}^4\text{He}({}^3\text{He}, \gamma){}^7\text{Be}$, ${}^7\text{Li}(p, \alpha){}^4\text{He}$, and ${}^7\text{Be}(n, p){}^7\text{Li}$ would be very valuable.

2.4 *Variations on a Theme*

As outlined by Wagoner (1973, 1974), the standard model rests on two fundamental and several auxiliary assumptions. The fundamental assumptions that define the general class of models studied are as follows:

1. Gravitation is described by a metric theory.
2. During the epoch of interest (nucleosynthesis), that portion of the Universe observed today (e.g. the Galaxy, the Local Group, extragalactic H II regions, etc.) was reasonably homogeneous and isotropic.

The geometry of the Universe is thus described by the Robertson-Walker metric. Some additional assumptions define the “standard” model:

3. The Universe was at a sufficiently high temperature that statistical equilibrium existed among all particles present.
4. Only the known particles were present (e.g. $N_v = 3$), and magnetic fields were negligible.
5. The baryon-to-photon ratio (“the baryon number of the Universe”) is positive (i.e. $n_{\bar{B}} \ll n_B = \eta n_\gamma$).
6. All particles were nondegenerate (e.g. $n_{\bar{\nu}} - n_\nu \ll n_\gamma$).
7. General relativity is valid.

The results presented above follow if these assumptions are adopted. The possible variations on the theme of the standard model are too numerous for us to attempt a complete catalog here. There are, however, several classes of models that deviate from the standard model in a well-defined fashion and that have been studied in some detail. We outline here the effects on the predicted abundances of such variations and later, when we compare with the observational data, place constraints on (or eliminate the possibility of) such deviations from the standard model.

2.4.1 NEW PARTICLES As Shvartsman (1969) first noted, a change in the energy density (at a fixed temperature) during nucleosynthesis will affect the expansion rate and, through the competition with the weak interaction rate, modify the yield of the ^4He (as well as the other light elements). Any species of light ($m \ll 1$ MeV) particle that is relativistic at the epoch of nucleosynthesis contributes to the total energy density (see Equations 8 and 13):

$$\rho_R = \left(\frac{g_{\text{eff}}}{2} \right) \rho_\gamma = \left[\frac{43}{8} + \frac{7}{8} (N'_v - 3) \right] \rho_\gamma. \quad 15.$$

The standard model counts, among the light particles, γ 's, e^+ 's, and three families of light, two-component neutrinos (e , μ , and τ), so that $g_{\text{eff}} = 43/4$ and $N'_v = 3$. Any additional families of leptons with *light* neutrinos or any

other exotic *light* particles (e.g. axions, gravitinos, photinos, etc.) will increase the total energy density (at a fixed temperature) over the standard value, and the Universe will expand (during the epoch of nucleosynthesis) more rapidly (Steigman et al. 1977):

$$t/t' = (\rho'_R/\rho_R)^{1/2} = \xi = [g_{\text{eff}}/(43/4)]^{1/2}. \quad 16.$$

We have already emphasized that the abundances of D and ^3He depend on the ratio η/ξ ; for fixed nucleon abundance, a faster expansion rate allows the survival of more D and ^3He . For modest speedup factors ($0 < \xi - 1 < 1$), the predicted abundances are those that in the standard model ($\xi = 1$) would correspond to a slightly lower nucleon abundance ($\eta' = \xi^{-1}\eta$). However, given the uncertainties associated with inferring the primordial abundances of D and ^3He from the observational data, little can be learned about ξ from the study of D and ^3He . A similar conclusion holds for ^7Li as well (Yang et al. 1979, hereafter YSSR).

In contrast, the ^4He mass fraction, which is relatively insensitive to the nucleon abundance ($\Delta Y_p \approx 0.011\Delta\eta/\eta$), can provide a probe of the early expansion rate. For modest speedup factors ($\xi - 1 < 1$; see OSSTY for details), more neutrons survive until nucleosynthesis begins in earnest, resulting in the production of more ^4He . If the synthesis of too much ^4He is to be avoided, the actual expansion rate during the epoch of nucleosynthesis cannot exceed by much that predicted in the standard model. A bound to the speedup factor ξ is, of course, equivalent to a bound to N'_ν , the number of light, two-component “equivalent” fermions (see Equation 13). For a fixed nucleon abundance η , we have $\Delta Y_p \approx 0.013(N'_\nu - 3) \approx 0.16(\xi - 1)$. Since in practice the permitted range of η is large, it is of value to evaluate Y_p at fixed $[(D + ^3\text{He})/H]_p$ (see Equation 14). In this case, we have $\Delta Y_p \approx 0.014(N'_\nu - 3) \approx 0.17(\xi - 1)$.

In counting relativistic particles, we have assumed that each neutrino with $m_\nu \ll 1$ MeV is “light” (i.e. counts as one, two-component fermion). We ignore the contribution from any “heavy” neutrinos if $m_\nu \gg 1$ MeV. How heavy is heavy and how light is light? Kolb & Sherrer (1982) have examined this question in detail and find that neutrinos with $m_\nu < 0.1$ MeV are “light” in the sense that $\Delta N_\nu = 1$. However, a neutrino species with $0.1 < m_\nu$ (MeV) < 10 – 15 contributes *more* than one equivalent neutrino ($\Delta N_\nu > 1$). For a neutrino species with 10 – $15 \leq m_\nu$ (MeV) ≤ 25 , Kolb & Sherrer (1982) find that $1 > \Delta N_\nu > 0.5$; heavy neutrinos only make a negligible contribution ($\Delta N_\nu \rightarrow 0$) for $m_\nu \gg 25$ MeV. We note that if the τ -neutrino is “heavy” ($m_{\nu\tau} \gg 25$ MeV), then the standard model should have $N_\nu = 2$.

The massive, electroweak gauge boson—the Z^0 —will decay into all neutrino species with $m_\nu < M_{Z^0}/2$. The measured width of the Z^0 will, therefore, provide a limit on the number of neutrino species that complements that from primordial nucleosynthesis (Schramm & Steigman

1984). The width of the Z^0 is sensitive to particles that would not be counted in primordial nucleosynthesis because they are too heavy ($m \gg 25$ MeV), *provided* that these particles are not *too* heavy ($m < M_{Z^0}/2$) and that they couple directly to the Z^0 . In contrast, the ${}^4\text{He}$ mass fraction is sensitive *only* to light particles ($m < 25$ MeV) *but* is subject to almost no restriction on their couplings. [Of course, if $T_{F,B} \ll T_\nu$, such particles would contribute negligibly; see Equation 13 (Steigman et al. 1979, Olive et al. 1981a).]

2.4.2 ANISOTROPIC EXPANSION Small deviations from perfect isotropy will, if present during the epoch of nucleosynthesis, increase the average expansion rate ($\xi > 1$) and hence tend to increase the predicted ${}^4\text{He}$ mass fraction (Hawking & Tayler 1966, Thorne 1967, Carswell 1969, Novikov 1971). If overproduction of ${}^4\text{He}$ is to be avoided, then the allowed anisotropy is severely restricted (Barrow 1976, 1977, Olson 1978). Recently, Rothman & Matzner (1984) have reinvestigated helium synthesis in anisotropic cosmologies including several effects that had not been included in earlier work. Despite the existence of competing processes, they find in all cases that ${}^4\text{He}$ increases sharply with anisotropy—even more dramatically than if time-scale effects alone are accounted for (R. Matzner, private communication to GS, 1984).

2.4.3 ALTERNATE THEORIES OF GRAVITY Many alternative theories of gravity that are sufficiently close to that of general relativity so that they agree with solar system tests may predict exceedingly different cosmological histories from the evolution described by the standard model. Primordial nucleosynthesis provides a strong-field test of gravitational theories (Will 1984).

2.4.3.1 Brans-Dicke theory Nucleosynthesis constraints to the scalar-tensor theory of gravity proposed by Brans & Dicke (1961) have been investigated by Greenstein (1968), Dicke (1968), Steigman (1976), Barrow (1978), and YSSR. As Will (1984) notes, to satisfy solar system tests, the Brans-Dicke coupling constant must be very large ($\omega > 200$). For ω so large, Brans-Dicke theory differs from general relativity by corrections of the order of ω^{-1} (Will 1984). For ω this large the speedup factor is $\xi \approx 10^{0.02}$, or $\xi - 1 \approx 0.05$ (YSSR); such a speedup is equivalent to $\Delta N'_\nu \approx 0.6$.

2.4.3.2 Variable-mass theory The theory proposed by Bekenstein (1977) has been studied by Bekenstein & Meisels (1980) and Meisels (1982), who found that it cannot account for the “large number” puzzle and be consistent with helium synthesis.

2.4.3.3 Varying G models Since the expansion rate depends on the Newtonian gravitational constant ($t^{-1} \propto G^{1/2}$), primordial nucleosynthesis

provides a constraint on the possible variation of G over cosmological epochs (Steigman 1976, Barrow 1978, YSSR). YSSR find that if $G \propto t^{-x}$ (and if all other physics is unchanged), then $x < 0.005$.

2.4.4 INHOMOGENEOUS MODELS Adiabatic density fluctuations (ρ_R varies spatially but $\eta = N/\gamma$ is constant) were investigated by Gisler et al. (1974). When such fluctuations have sizes greater than that of the causal horizon at the epoch of nucleosynthesis, they evolve like separate universes and do not produce large differences from the standard model (for the same value of η). However, on scales smaller than the horizon, adiabatic fluctuations behave like sound waves and can lead to different primordial abundances from the standard model (Olson 1978). Recently, Matzner (1984) has studied nucleosynthesis in a cosmology with strong ($\delta\rho/\rho > 5$) adiabatic fluctuations on scales comparable to the horizon at the epoch of nucleosynthesis. Since the horizon size at nucleosynthesis is quite small, different horizon regions are completely mixed at present. Matzner (1984; private communication, 1984) finds that slightly more ${}^4\text{He}$ is produced ($\Delta Y_p \approx 0.01$) as a function of the D and/or ${}^3\text{He}$ abundance as compared with the amount produced in the standard model (see Figure 3).

Isothermal density fluctuations (ρ_R spatially constant, η varying) have been considered by Wagoner (1973), Epstein & Petrosian (1975), Barrow & Morgan (1983), and YTSSO. In low- η regions, D and ${}^3\text{He}$ are enhanced and ${}^4\text{He}$ is reduced (see Figure 2); in high- η regions, D and ${}^3\text{He}$ are negligible and ${}^4\text{He}$ is abundant. As above, to compare with observational data, many horizon volumes must be averaged. YTSSO find that $\langle\eta_{10}\rangle > 3\text{--}4$ and $\delta\eta/\eta < 1.4\text{--}1.7$ if $\langle Y_p \rangle < 0.25$ and $\langle (D + {}^3\text{He})/H \rangle < 6\text{--}10 \times 10^{-5}$.

2.4.5 NEUTRINO DEGENERACY Although the universal baryon asymmetry is very small ($n_B - n_{\bar{B}} = \eta n_\gamma < 10^{-9} n_\gamma$), the lepton asymmetry need not be. Neutrino degeneracy—an excess of neutrinos over antineutrinos, or vice versa—will affect primordial nucleosynthesis in two ways. The excess density (compared with the density of the standard, nondegenerate case) causes a speedup in the expansion rate, leading to enhanced production of D, ${}^3\text{He}$, and ${}^4\text{He}$. For electron-neutrino degeneracy there is a second, more important effect. The neutron-proton interconversion reactions are modified by e-neutrino degeneracy. For example, suppose there is an excess of e-neutrinos over anti-e-neutrinos. (This corresponds to a positive chemical potential for the e-neutrinos μ_{ν_e} .) Then, in the reactions $p + e^- \leftrightarrow n + \nu_e$, the equilibrium is shifted toward a lower n/p ratio. For $\mu_{\nu_e} < 0$, the excess of anti-e-neutrinos drives the n/p ratio to higher values through the reactions $p + \bar{\nu}_e \leftrightarrow n + e^+$. In the presence of e-neutrino degeneracy, the equilibrium n/p ratio is

$$n/p = \exp [-(\Delta m + \mu_{\nu_e})/kT]. \quad 17.$$

As the Universe expands and cools, the ratio $\xi_v \equiv \mu_v/kT_v$ remains constant; the degeneracy parameter ξ_v is not to be confused with the speedup factor ξ . For $|\xi_{ve}| > 1$ (compared with $\xi_{ve} = 0$ for the standard model), the neutron abundance at nucleosynthesis can be altered dramatically, leading to quantitatively and qualitatively different predictions for the primordial abundances of the light elements.

The effects of neutrino degeneracy were first studied by Wagoner et al. (1967) and subsequently by Beaudet & Goret (1976), Yahil & Beaudet (1976), Beaudet & Yahil (1977), David & Reeves (1980), Fry & Hogan (1982), and Steigman (1985). By requiring that neutrino degeneracy not spoil the good agreement between the predictions of the standard model and the observational data, the most restrictive constraints on a possible universal lepton asymmetry are found. For example, to avoid overproducing D and ^4He when μ - and/or τ -neutrinos are degenerate leads to the constraint (Steigman 1985) $|\xi_v| < 1.4\text{--}1.7$ (for $\text{D}/\text{H} < 10^{-4}$ and $Y_p \leq 0.25\text{--}0.26$). A much lower bound to e-neutrino degeneracy follows from similar comparisons (Steigman 1985). For example, if we require $Y_p > 0.23$ (0.22), then $\xi_{ve} < 0.10$ (0.15); for $Y_p < 0.25$ (0.26), $\xi_{ve} > -0.05$ (-0.06).

If two or more neutrino species are degenerate—but with unequal degeneracy parameters—a much wider range of possibilities is available. In such a situation the yields of primordial nucleosynthesis will depend on three free parameters: the nucleon abundance η , the electron degeneracy ξ_{ve} , and the speedup factor ξ . It may not be surprising that for appropriate choices of these three parameters, we may be able to reproduce the predictions of the standard model (which depend on only the parameter η , since $\xi_{ve} = 0$ and $\xi = 1$ for the standard model). For example, for η fixed and $\xi_{ve} > 0$, less D, ^3He , and ^4He will tend to be synthesized, since fewer neutrons are available. However, if in addition the expansion rate is speeded up (above the speedup accompanying $\xi_{ve} > 0$), this compensating effect, which tends to increase the abundances of D, ^3He , and ^4He , may result in abundances indistinguishable from those in the standard model. Degeneracy in e- and μ - or τ -neutrinos can compensate for changes in nucleon abundance and/or in the number of light species. Therefore, nucleosynthesis constraints on η and N'_v are only valid in the absence of degeneracy.

Since the primordial abundance of ^7Li depends on the competition among several competing production and destruction rates, the behavior of $^7\text{Li}/\text{H}$ in the presence of neutrino degeneracy is more complicated than that of the other light elements (David & Reeves 1980, Steigman 1985). Accurate determinations of the primordial abundance of ^7Li can help exclude degenerate models that otherwise would not be in conflict with the abundances of the light elements.

Later, when we compare the abundances derived from the observational data with those predicted by the standard model, we will be led to a low (nucleon) density universe ($\eta_{10} < 10$). The (nucleon) mass density of such a model fails—by at least a factor of 5—to “close” the Universe [$\rho_N < (1/5)\rho_c$]. David & Reeves (1980) have explored the possibility that indeed $\rho_N = \rho_c$ ($\eta_{10} \approx 50$), but that e- and μ - or τ -neutrinos are degenerate. With the appropriate choices of $\xi_{\nu e}$ and $\xi_{\nu\mu}$, they find that consistency with the data is possible. Since the work of David & Reeves (1980), the new observations of lithium in Pop II stars (Spite & Spite 1982a, Spite et al. 1984) have probably lowered considerably the estimate of the primordial abundance of ${}^7\text{Li}$. Steigman (1985) has reinvestigated whether $\eta_{10} > 50$ can be consistent with the observed abundances and has concluded that for speedup factors $\xi < 7$, there is *no* consistency with the abundances of all the light elements for *any* value of $\xi_{\nu e}$. For $\xi > 7$ and $\eta_{10} \approx 50$, the Universe remains radiation dominated (by relativistic degenerate neutrinos) down to a redshift of order 100. In such a model there is insufficient time for perturbations—given the absence of observable fluctuations in the microwave background radiation—to grow into the observed large-scale structure of the present Universe. Neutrino degeneracy cannot “save” a critical-density, nucleon-dominated universe.

3. OBSERVED ABUNDANCES

3.1 *Destruction and Production During Galactic Evolution*

The abundances of the elements we observe today are affected by nuclear processing in stars. The general chemical enrichment through galactic and stellar evolution not only changes abundances, but it also affects the physics of stellar interiors and atmospheres and of the interstellar medium. Even the oldest stars may reveal, for example, the products of nuclear reactions and mixing and the effects of gravitational settling on the abundances measured in their surface layers. A general overview is presented here, and more specific details are discussed in the subsequent sections.

Primordial D is readily destroyed in stars wherever the temperature is greater than $\sim 6 \times 10^5$ K, primarily by (p, γ) reactions. In effect, this means that D can be found only in the envelopes of stars hotter than B8 ($M > 3.5 M_\odot$) because it is destroyed during the pre-main-sequence phase of lower-mass stars while they are fully convective (Bodenheimer 1966). Other initial conditions and different physics have been used by Mazzitelli & Morretti (1980) that result in greater pre-main-sequence depletion in higher-mass models. Models of the chemical evolution of the Galaxy (e.g. Audouze & Tinsley 1976) suggest that the present amount of D is about

0.4 times the primordial amount (but see Gry et al. 1983b). Such estimates are fraught with more than the usual uncertainties because they require knowledge of the birth rate function, the initial mass function, mass loss rates in various stages of stellar evolution, infall to and mixing in the galactic disk, the composition of the infalling material, etc.

Deuterium is converted to ^3He in stars, some ^3He is destroyed in stars, and new ^3He is created in low-mass stars and produces a peak in the outer regions at the base of the red giant branch (Iben 1967, Rood et al. 1976). Mass loss from red giants may enrich the present interstellar content above the protosolar and primordial amounts.

Helium-4 is a primary product of stellar energy generation. Throughout stellar evolution a star becomes more and more enriched in ^4He . Through stellar mixing and mass loss, the interstellar gas can increase its proportion of ^4He . [For reviews of stellar He processing in massive stars and in low- and intermediate-mass stars, see Maeder (1983) and Renzini (1983), respectively.] The least-processed environments, then, should preferentially contain a more nearly primordial abundance of ^4He .

Nuclear reactions with protons destroy Li in low-mass stars during pre-main-sequence evolution (Bodenheimer 1965), and apparently during the main-sequence phase through deep circulation (e.g. Straus et al. 1976, Vauclair et al. 1978); the observed surface abundance is further reduced by dilution in red giants (Iben 1965, 1967). Many sources for the production of Li have been identified, including supernovae (Audouze & Truran 1973, Arnould & Nørgaard 1975), supermassive objects (e.g. Nørgaard & Fricke 1976), novae (Starrfield et al. 1978; see also Vigroux & Arnould 1979), red giant interiors (Cameron 1955, Cameron & Fowler 1971, Scalo & Ulrich 1973, Sackmann et al. 1974, Scalo et al. 1975, Dean et al. 1977), solarlike flares (Canal 1974, Canal et al. 1975, 1980), and galactic cosmic-ray spallation (Meneguzzi et al. 1971, Meneguzzi & Reeves 1975).

3.2 *Deuterium*

As can be seen in Figure 2 the amount of D is very sensitive to the nucleon abundance: At high η , D is rapidly converted to ^3H , ^3He , and ^4He through various nuclear reactions. Deuterium could *potentially* provide the most important constraint on Big Bang cosmology. Any additional D that is produced in stellar nuclear reactions is destroyed in stellar interiors by the energy-generating reactions, so that the observed abundances provide a lower limit on the primordial D abundance. The observational situation has been discussed in several recent reviews; among them are Audouze (1984), Ferlet et al. (1985), Geiss & Reeves (1981), Laurent (1983), and Vidal-Madjar (1983).

The major approach to searching for D has been through the isotropic

shift of atomic H I: This approach has been used in stellar atmospheres at H α and in the interstellar gas in the Lyman lines. Molecular spectra of deuterated molecules are observed in planetary atmospheres and in interstellar space. Radio observations to find the D I analog of the H I 21-cm line at a wavelength of 91.6 cm are extremely difficult, and the interpretation is not straightforward; a marginal detection by Cesarsky et al. (1973) and Pasachoff & Cesarsky (1974) toward the galactic center could not be confirmed by Sarma & Mohanty (1978) or Anantharamaiah & Radhakrishnan (1979).

3.2.1 STELLAR Although stellar D has not been detected, interesting upper limits have been found that may contain information on the depletion of D in stars and thus provide guidance for the galactic chemical evolution of deuterium. Early searches for stellar D were conducted by Peimbert & Wallerstein (1965); more recently, Peimbert et al. (1981) and Ferlet et al. (1983) have reduced the upper limit in Canopus. Here, we take $D/H < 1 \times 10^{-6}$ as a conservative stellar limit for comparisons with the amount of D found in interstellar gas.

3.2.2 INTERSTELLAR TOWARD HOT STARS One of the many significant contributions of the Copernicus satellite was the detection of interstellar D in the wings of the Lyman lines of H I along the lines of sight to several nearby cool stars and to more distant O and B stars. The higher Lyman lines (L β , L γ , L δ , and L ϵ) are studied in the interstellar spectra of the O and B stars; interstellar L α is too strong for D α to be distinguished. Stars with high values of $v \sin i$ are observed to minimize the complications of the stellar line profile shape. The first detection was by Rogerson & York (1973), followed by York & Rogerson (1976); their five lines of sight gave an average value of $D/H = 1.6 \times 10^{-5}$. Further investigations toward eight other O and B stars have been made by Vidal-Madjar et al. (1977), Laurent et al. (1979), Ferlet et al. (1980), Vidal-Madjar et al. (1982), and York (1983).

There are at least two complications in the derivation of interstellar D/H values: stellar contamination of the interstellar profile, and multiple clouds in the line of sight. Recently, a suggestion by Vidal-Madjar et al. (1983) that the D I lines toward ϵ Per may be contaminated by high-velocity gas of stellar H I has been discussed by Gry et al. (1983a). They have presented evidence of small profile changes on time scales of hours in the L γ and L δ lines in the spectrum of ϵ Per that they attribute to high-velocity "puffs" of H I in the stellar wind. The strength of the H I features vary, but unfortunately the ones near -80 km s^{-1} blend with the expected D I features. Under these rare conditions, the derived D/H abundance would be too high. Further work by Gry et al. (1984) supports the existence of some transient components in other O and B stars. They are seen in the stars of luminosity

DELTA ORIONIS

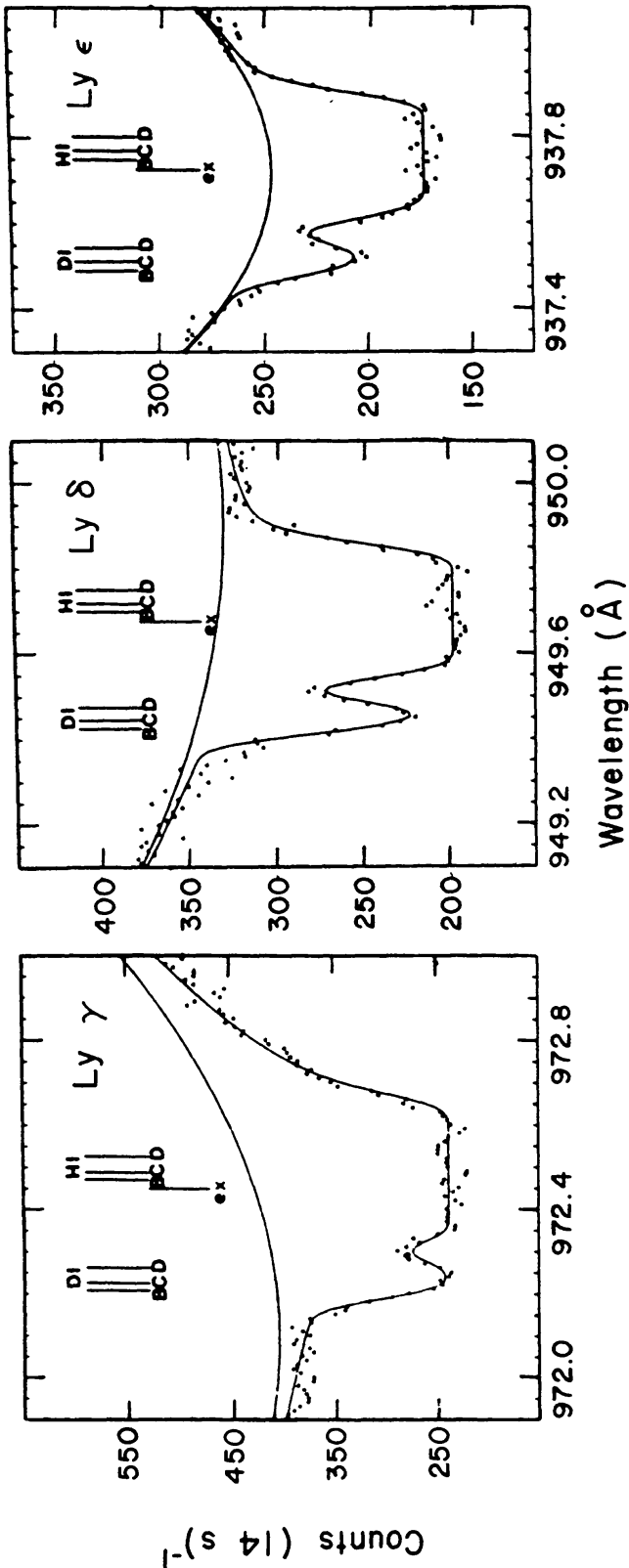


Figure 4 Observed Copernicus spectra (dots) of the Ly, Lδ, and Lε features of δ Ori and the calculated profiles (solid lines) for the H I and D I lines arising in multiple cloud components labeled B, C, and D. (After Laurent et al. 1979.)

classes III and IV, but not in classes I and II, in the eight stars they studied.

The presence of multiple interstellar clouds along the line of sight complicates the analysis because the multiple components are blended in the UV D I spectrum. High-resolution optical observations of individual lines, e.g. Na I, from the separate clouds provide guidance. Especially detailed analyses of multiple clouds have been made for δ Ori, ε Ori, and ι Ori by Laurent et al. (1979), for γ Cas by Ferlet et al. (1980), and for λ Sco by York (1983). An example for δ Ori from Laurent et al. (1979) is shown in Figure 4. This work shows how complex the cloud and line structure can be. The Orion region is particularly complex, as Hobbs' (1969) Na I observations show, with many clouds along the 400–500 pc line of sight. Those clouds would be unresolved by the Copernicus observations, the parameter b assigned for the Doppler velocity would be too high, and the D/H value would be underestimated. The nearest B stars with the least-complicated lines of sight are β Cen, α Vir, and λ Sco, and the mean D/H value is 1.2×10^{-5} . Results collected from all sources are shown in Figure 5. This figure and the results for the "cleanest" lines of sight show that the most probable D/H value lies between 0.8 – 2.0×10^{-5} , but values outside this range cannot be excluded.

3.2.3 INTERSTELLAR TOWARD COOL STARS The evaluation of D/H toward nearby cool stars is complicated by the necessity to have accurate knowledge of the photospheric and chromospheric stellar H-line profile. Only the interstellar $L\alpha$ line is strong enough to be observed in the nearby stars. A fine example of an observed spectrum, Capella (α Aur, G5 III), is shown in Figure 1 of Dupree et al. (1977). A schematic version of the

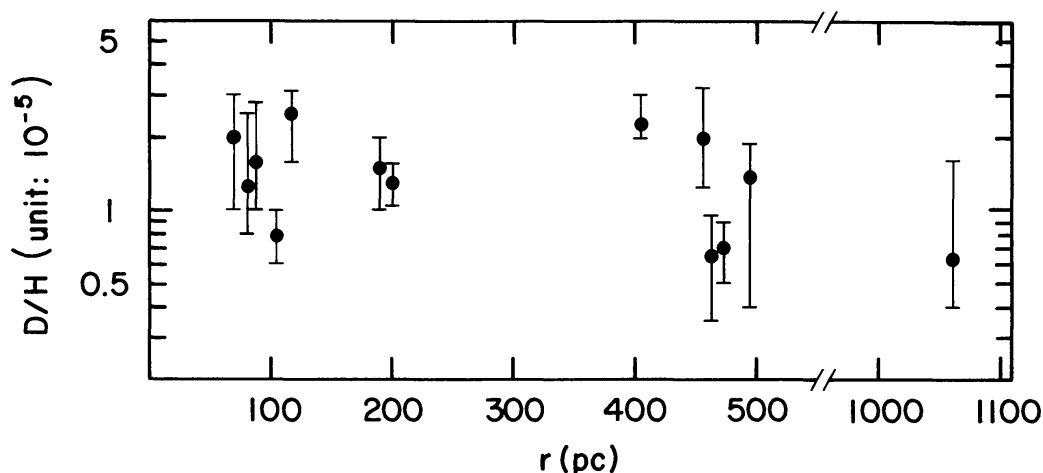


Figure 5 Observed D/H ratios inferred for the interstellar medium toward hot stars. The distances on the x-axis are uncertain, but they serve to spread out the data points. (The basic data are from Laurent 1983.)

combined stellar plus interstellar, H I $L\alpha$ plus D I $L\alpha$ spectrum is shown in Figure 6, taken from McClintock et al. (1978). These figures illustrate the difficulty of extracting accurate D/H values from the cool star spectra. The first attempt was by Dupree et al. (1977), who studied α Cen A (G2 V) at 1.3 pc and α Aur (G5 III) at 14 pc and found values of $D/H = 2.4 \times 10^{-6}$ and 3.9×10^{-5} , respectively: These are more than an order of magnitude different for the local interstellar gas. Subsequently, McClintock et al. (1978) added two more nearby stars, ϵ Eri (K2 V) and ϵ Ind (K5 V), and

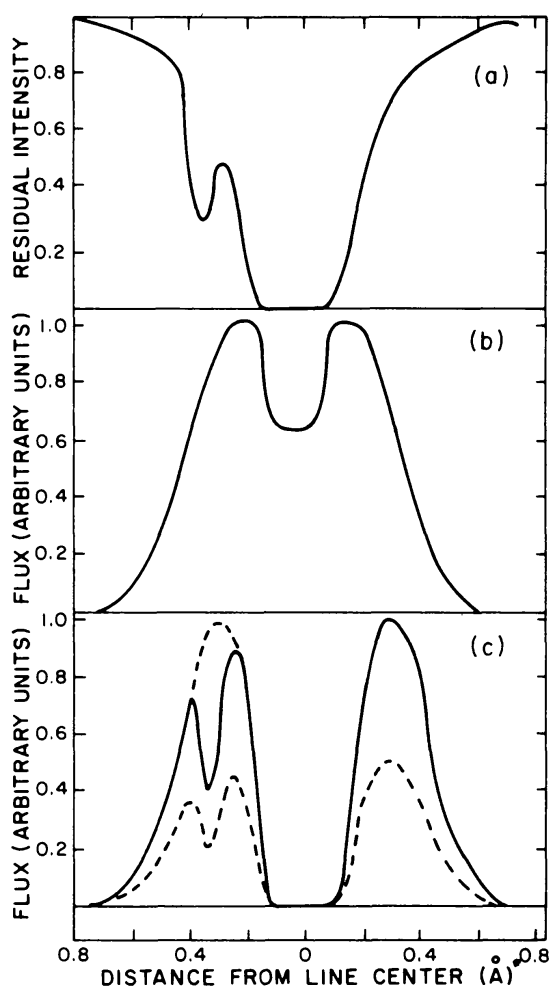


Figure 6 An example of the complexity of determining D/H from the interstellar gas along the line of sight to cool stars. The upper panel (a) is a schematic interstellar H plus D absorption profile. The middle panel (b) shows the assumed $L\alpha$ stellar (chromospheric) emission profile. The lower panel (c) shows the composite profile: The lower dashed curve results from the combination of the D and H interstellar absorption of the stellar emission, while the upper dashed curve shows the effect of interstellar H absorption only (no interstellar D). The solid curve is simply the lower dashed curve normalized to unit height. (From McClintock et al. 1978.)

reevaluated the Dupree et al. (1977) observations. They found a more homogeneous interstellar gas in the solar vicinity and D/H ratios near 1.8×10^{-5} . Other analyses of D/H from the spectra of nearby cool stars have been made of HR 1099 by Anderson & Weiler (1978), α CMi by Anderson et al. (1978), and λ And by Baliunas & Dupree (1979). These collected results are shown in Figure 7.

3.2.4 INTERSTELLAR DEUTERATED MOLECULES Although there exist extensive observations of deuterated molecules (DCO^+ , DCN , DNC , HDO , etc.) in the interstellar medium, such studies have shed virtually no light on the issues of the interstellar or primordial abundances of deuterium. The reason is that chemical and physical fractionation effects have led to enormous enhancements of D in various molecules. For example, Penzias (1979) finds that the ratio of DCO^+ to HCO^+ varies from 2×10^{-4} to 1.4×10^{-2} , and that of DCN to HCN from 1.4×10^{-3} to 1.2×10^{-2} . Even more dramatically, the ratio DNC/HNC is found by Snell & Wooten (1979) to be as large as 0.05 to 2.5. It is clear that such observations are of more relevance to interstellar chemistry than to the interstellar or primordial abundances of deuterium. The enormous variation in the molecular abundances should serve as a caution when deriving the solar system deuterium abundance from the abundances of deuterated molecules in the atmospheres of the giant planets. Indeed, as Geiss & Reeves (1981) note, the presolar nebula itself may have been enhanced in D.

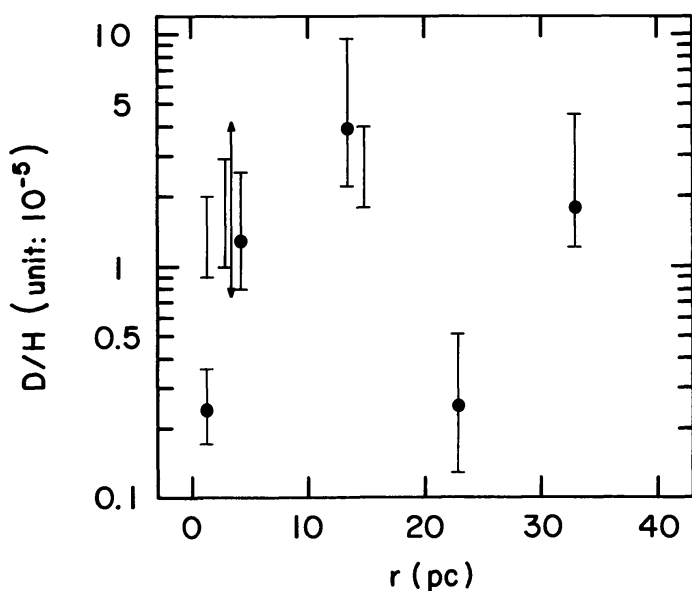


Figure 7 Observed D/H ratios inferred for the interstellar medium toward nearby cool stars. (The basic data are from Laurent 1983.)

3.2.5 INTERSTELLAR SUMMARY Both Figures 5 and 7 show a large scatter, beyond the individually assigned error bars. In both types of studies—toward more distant O and B stars and toward nearby cool stars—there are systematic errors. Furthermore, it is possible that there are local enrichments or depletions of D. For example, Bruston et al. (1981) demonstrate that the McKee & Ostriker (1977) model interstellar cloud could have regions depleted by factors of 2 and others enriched by factors of 10 due to radiation pressure and chemical fractionation. Different types of difficulties affect the data reduction, analysis, and interpretation for the derivation of the interstellar D/H ratio from the spectra of hot stars vs. cool stars, but the quality of the data and the analysis techniques seem more reliable for the hot stars. Our preferred range of possible values for the interstellar gas is $D/H = 0.8\text{--}2.0 \times 10^{-5}$.

3.2.6 SOLAR SYSTEM Values of D/H found in the Earth and meteorites are substantially higher (by factors of 4–40) than those measured in the atmospheres of the giant planets and inferred from ^3He in the gas-rich meteorites and the solar wind (see Section 3.3); this difference is due to the effects of fractionation at low temperatures (Black 1971, 1973, Geiss & Reeves 1972, 1981). The observed D/H values in Jovian planets will be representative of the early solar nebula if D was not transformed to ^3He during the formation of the solar system. The molecular ratios of HD/H_2 and $\text{CH}_3\text{D}/\text{CH}_4$ have been used to deduce D/H, but such estimates are dependent on characteristics of the temperature and pressure structure, convective processes, details of the chemistry including the possible presence of dust, and in the case of the methane studies, knowledge of the planetary C abundance.

Kunde et al. (1982) have reviewed the observations of D/H in the solar system, especially from the giant planets, in connection with their analysis of the gas composition of Jupiter's troposphere and of the CH_3D (at 5 and 8.6 μm) and CH_4 (at 7.7 μm) observations from the Voyager I Infrared Interferometer Spectrometer (IRIS). A sample of the IRIS Jupiter data and the synthetic spectra of Kunde et al. is shown in Figure 8. These Voyager I data result in a value of $D/H = 3.6 \times 10^{-5}$ from the methane absorption-band analysis. Encrenaz & Combes (1982) have reexamined the results from HD and H_2 using new laboratory data and find the Jovian D/H range to be $1.2\text{--}3.1 \times 10^{-5}$ and a less certain result for Saturn of $2\text{--}15 \times 10^{-5}$. The results for Uranus of $D/H = 3\text{--}6 \times 10^{-5}$ reported by Trafton & Ramsay (1980) are similar. Gautier (1983) assesses the solar system results and concludes that the best value from the Voyager I data is $3.2^{+0.9}_{-1.25} \times 10^{-5}$, which is consistent with the Encrenaz & Combes results. Hubbard & MacFarlane (1980) argue that the amount of D present in the atmospheres of Jupiter and Saturn will be close to the presolar value.

3.2.7 DEDUCTION OF PRIMORDIAL DEUTERIUM The above discussion results in three different types of information about deuterium:

1. The present-day abundance from the interstellar studies is $8 \times 10^{-6} \leq \text{D}/\text{H} \leq 2 \times 10^{-5}$.
2. The pre-solar-system abundance (4.5×10^9 yr ago) obtained from the giant planet atmospheres is $1 \times 10^{-5} \leq \text{D}/\text{H} \leq 4 \times 10^{-5}$.
3. The stellar atmosphere value for a young, evolved star (F0 Ib) is $\text{D}/\text{H} < 10^{-6}$.

The question now is how to evaluate the amount of depletion of primordial D due to stellar and galactic evolution. Deuterium is particularly sus-

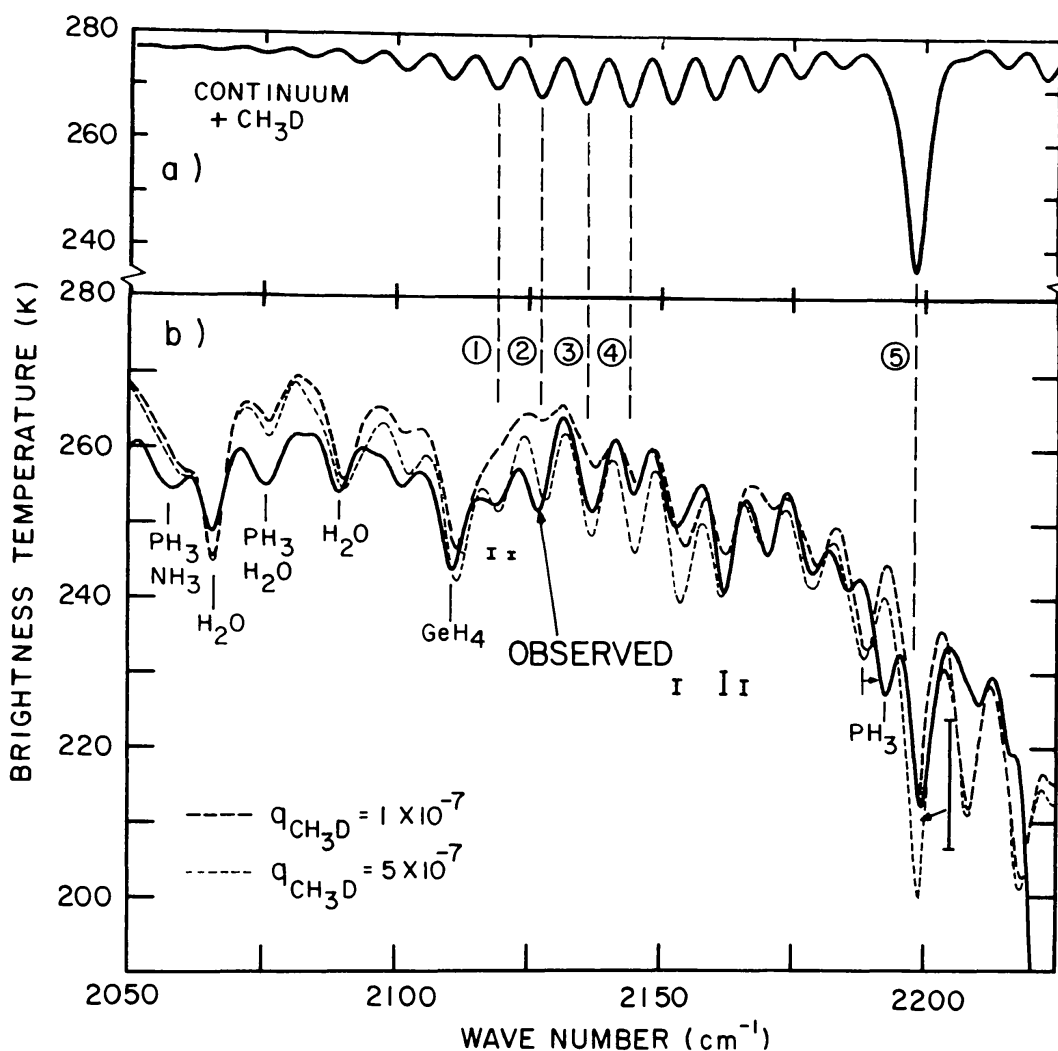


Figure 8 Comparison of observed and synthetic spectra in the deuterated methane (CH_3D) region from the Voyager I IRIS spectra of Jupiter's atmosphere. Panel (a) shows where the CH_3D features are located. The P-branch multiplets labeled 1–4 and the Q-branch feature labeled 5 were used to determine the mole fraction of CH_3D . (From Kunde et al. 1982.)

ceptible to destruction by nuclear reactions in matter at stellar densities having temperatures of $T > 10^5$ K. Audouze & Tinsley (1974) first tried to model the effects of evolution on the abundances of a number of light elements and isotopes, including D. They found that the D abundance was unlikely to change by more than a factor of 2–3. This issue has been reassessed by Gry et al. (1983b), who consider two basic models: one in which the gas falling into the galactic disk is essentially D-free, having been processed through stars; and the other in which the infalling gas contains the primordial composition. In the latter case, they again find about a factor of 2 reduction in the D abundance, while in the former the present-day D could be as much as a factor of 50 less than the primordial D/H ratio. More recent models on the chemical evolution of D have been done by Clayton (1985) and Delbourgo-Salvador et al. (1985).

The guidance that comes from the empirical results above suggests that stars do destroy D, since there is virtually no D in the atmosphere of Canopus, whose main-sequence predecessor was probably a B2 V star of $10 M_{\odot}$ (Peimbert et al. 1981). Further, the comparison of the present interstellar D with that in the protosolar nebula of 5 Gyr ago suggests a possible depletion, although the ranges in D/H values from these two sources do overlap. Over the lifetime of the galactic disk, with the fairly linear predictions with time of the models, depletions of 2 to 10 might be expected; such values are consistent with either type of model of Gry et al. (1983b). The combined uncertainties in the observations and the chemical models make the step back to the primordial abundance a particularly precarious one. We are able with some certainty to establish a lower limit for D/H from the interstellar observations and select a range of depletion factors to arrive at the primordial one. From the observed range of D/H taken from the interstellar values (item #1 above), a depletion from primordial to present D/H by a factor of 2 gives

$$1.6 \times 10^{-5} < (D/H)_p < 4 \times 10^{-5},$$

and a depletion by a factor of 10 gives

$$8 \times 10^{-5} < (D/H)_p < 2 \times 10^{-4}.$$

3.3 *Helium-3*

The value of ${}^3\text{He}$ as a probe of primordial nucleosynthesis is very unclear at present. Although ${}^3\text{He}$ is the product of incomplete hydrogen burning in the cooler outer regions of low-mass ($< 2 M_{\odot}$) stars (Iben 1967), ${}^3\text{He}$ is burned away in the interiors of heavier stars. However, *some* ${}^3\text{He}$ will survive in the outer layers of even these more massive stars (Dearborn et al. 1978). Since deuterium will be burned to ${}^3\text{He}$, the surviving ${}^3\text{He}$ will have

been augmented by the D incorporated in the star along with the original ^3He . In the course of galactic evolution there is, therefore, a competition between destruction, survival, and production (by conversion of D to ^3He as well as the synthesis of ^3He by incomplete H-burning). [See Delbourgo-Salvador et al. (1985) for a recent discussion of the evolution of D and ^3He .] Whether the protosolar and/or the present interstellar abundance of ^3He should be greater than, less than, or comparable to the primordial abundance is difficult to assess. The paucity of actual data on the interstellar abundance of ^3He exacerbates the problem.

3.3.1 SOLAR SYSTEM ABUNDANCE In the last 4.5 Gyr, the solar wind has implanted ^3He in the gas-rich meteorites, the lunar soil and breccias, and—more recently—in the foil placed on the Moon by the Apollo astronauts. Any presolar deuterium has, during the approach of the Sun to the main sequence, been burned to ^3He , so that the solar wind abundance of ^3He is representative of the presolar abundance of D *plus* ^3He . It should be noted, however, that the solar wind ^3He may have been contaminated by additional ^3He dredged up from the interior (Schatzman & Maeder 1981); it is difficult to estimate the importance of this effect (Michaud 1985). In the following we interpret the observations as a measurement of the presolar abundance of D plus ^3He ; since it is the $^3\text{He}/^4\text{He}$ ratio that is measured, the observations lead to a determination of $[(\text{D} + ^3\text{He})/^4\text{He}]_{\odot}$, the abundance ratio by number. In the gas-rich meteorites, Jeffrey & Anders (1970) find an abundance ratio of $3.79(\pm 0.40) \times 10^{-4}$. Black (1972), in a study of gas-rich meteorites, lunar soil, and breccias, obtains a value of $3.9(\pm 0.3) \times 10^{-4}$. From the lunar foil, Geiss et al. (1970) determine a value of $4.3(\pm 0.3) \times 10^{-4}$. Despite short-term variability in the $^3\text{He}/^4\text{He}$ ratio observed in the solar wind (see, for example, Geiss 1982), the long-term averages are very stable. If we average the above results, we obtain a value of $\langle (\text{D} + ^3\text{He})/^4\text{He} \rangle_{\odot} = 4.0(\pm 0.2) \times 10^{-4}$.

Jeffrey & Anders (1970) and Black (1971, 1972) noted that there was a second component of ^3He in the meteorites, which Black (1971, 1972) and Geiss & Reeves (1972) interpreted as presolar ^3He uncontaminated by the burning of presolar D to ^3He . This component is particularly clear in the carbonaceous chondrites, which provide a sample of the primitive material of the presolar nebula. If this interpretation of the data is accepted, the ^3He abundance in the carbonaceous chondrites provides an estimate of the presolar abundance of ^3He . In their pioneering work, Jeffrey & Anders (1970) found that $(^3\text{He}/^4\text{He})_{\odot} = 1.43(\pm 0.40) \times 10^{-4}$, and Black (1972) obtained a value of $1.5(\pm 1.0) \times 10^{-4}$. More recent determinations of higher statistical accuracy have been made by Frick & Moniot (1977) [$1.558(\pm 0.055) \times 10^{-4}$] and by Eberhardt (1978) [1.460

$(\pm 0.073) \times 10^{-4}$]. An average (weighted) of all the data suggests that $\langle {}^3\text{He}/{}^4\text{He} \rangle_{\odot} = 1.54(\pm 0.27) \times 10^{-4}$; an average of the most recent results is $1.54(\pm 0.05) \times 10^{-4}$.

If the interpretation of the origin of the two observed ${}^3\text{He}/{}^4\text{He}$ ratios is correct, and if the solar wind ${}^3\text{He}$ is not significantly contaminated by ${}^3\text{He}$ dredged up from the solar interior, then an estimate of the presolar abundance of deuterium may be made: $(\text{D}/{}^4\text{He})_{\odot} = [(\text{D} + {}^3\text{He})/{}^4\text{He}]_{\odot} - ({}^3\text{He}/{}^4\text{He})_{\odot}$. If all the data are averaged, then $\langle \text{D}/{}^4\text{He} \rangle_{\odot} = 2.5(\pm 0.5) \times 10^{-4}$; if we limit ourselves to the highest (statistical) accuracy results, we obtain $\langle \text{D}/{}^4\text{He} \rangle_{\odot} = 2.49(\pm 0.24) \times 10^{-4}$.

To derive the presolar abundances—relative to H—of D and ${}^3\text{He}$, we must know the solar abundance of ${}^4\text{He}$. Unfortunately, $({}^4\text{He}/\text{H})_{\odot} (= y_{4\odot})$ is only poorly known (see the discussion in Section 3.4.5). In converting the meteoritic ${}^3\text{He}/{}^4\text{He}$ ratios to presolar D/H and ${}^3\text{He}/\text{H}$ ratios we *adopt* $y_{4\odot} = 0.09 \pm 0.01$ (although our best “guess” would be $y_{4\odot} \approx 0.10$). The meteoritic and lunar data, along with an estimate of the solar helium abundance, permit us to estimate the presolar abundances of D and ${}^3\text{He}$:

$$[(\text{D} + {}^3\text{He})/\text{H}]_{\odot} = 3.6(\pm 0.6) \times 10^{-5}, \quad 18a.$$

$$({}^3\text{He}/\text{H})_{\odot} = 1.4(\pm 0.4) \times 10^{-5}, \quad 18b.$$

$$(\text{D}/\text{H})_{\odot} = 2.2(\pm 0.7) \times 10^{-5}. \quad 18c.$$

Notice that this *indirect* determination of the presolar abundance of deuterium is in excellent agreement with the more direct determinations from the studies of deuterated molecules in Jupiter (reviewed earlier in Section 3.2.6).

3.3.2 INTERSTELLAR ABUNDANCE Singly ionized ${}^3\text{He}$ can be observed by its 8.7-GHz hyperfine line—the analog of the 21-cm spin-flip line in neutral hydrogen. Since ${}^4\text{He}$ has no hyperfine structure, there is no confusion with a corresponding ${}^4\text{He}$ line. In H II regions the ${}^3\text{He}^+$ transition is optically thin and collisionally excited. The weakness of the line and the small line-to-continuum ratio make it very difficult to determine the ${}^3\text{He}^+$ abundance reliably. Early efforts by Predmore et al. (1971) produced only upper limits. Rood et al. (1979) reported an observation in the H II region W51, which was confirmed by Wilson & Rood (1979). More recently, a heroic effort by Rood et al. (1984) has borne fruit. In a study of six galactic H II regions, they report detections of ${}^3\text{He}^+$ in W3, W51, and W43; for Orion A, W49, and M17S, Rood et al. only have upper limits. Even with a reliably measured line strength for ${}^3\text{He}^+$, it is far from trivial to derive a meaningful ${}^3\text{He}/\text{H}$ ratio, since the amount of H^+ in the beam (which depends on n_e^2 integrated

through the H II region and thus is sensitive to inhomogeneities in source structure) must be determined. Rood et al. (1984) discuss clearly the observational and modeling uncertainties affecting their results.

The upper limits found by Rood et al. (1984) for Orion A (${}^3\text{He}/\text{H} < 6 \times 10^{-5}$) and W49 and M17S (${}^3\text{He} < 2 \times 10^{-5}$), as well as the detection in W43 (${}^3\text{He}/\text{H} \approx 4 \times 10^{-5}$), are comparable to the estimates of the presolar ${}^3\text{He}$ abundance discussed above. The abundance estimate for W51 (${}^3\text{He}/\text{H} \approx 8 \times 10^{-5}$) exceeds the solar system value by a factor of 2–4. Most surprising, however, is the very large result found for W3: ${}^3\text{He}/\text{H} \approx 40 \times 10^{-5}$. As Rood et al. (1984) emphasize, such a large range of ${}^3\text{He}$ abundances is very difficult to account for. With due regard for the uncertainties in the solar system and H II region abundance determinations, there is, nonetheless, the suggestion that the galactic abundance of ${}^3\text{He}$ has increased in the last 4.5×10^9 yr.

3.3.3 EVOLUTION OF ${}^3\text{He}$ If the ${}^3\text{He}$ produced in the outer layers of the low-mass stars (Iben 1967, Rood 1972) survives the late stages of stellar evolution (thermal pulses, He flashes, etc.) and is ejected, stellar production alone might be a sufficient source of the presolar abundance (Talbot & Arnett 1973). However, if sufficient deuterium is produced primordially to account for the presolar value [$(\text{D}/\text{H})_{\text{p}} > 1 \times 10^{-5}$], then the Big Bang synthesizes enough ${}^3\text{He}$ to account for that presolar value ($[{}^3\text{He}/\text{H}]_{\text{p}} > 1 \times 10^{-5}$; see Figure 2 and Table 1) (Audouze & Tinsley 1974, Tinsley 1977).

Rood et al. (1976) noted that since low-mass stars are potentially important sources of newly synthesized ${}^3\text{He}$, the epoch since the formation of the solar system may have been one in which the galactic abundance of ${}^3\text{He}$ increased dramatically. They found the “embarrassing” result that, in the absence of destruction or dilution, the present enrichment rate is so large that the interstellar abundance of ${}^3\text{He}$ would exceed the solar system abundance in less than a billion years. By modeling the recent (since the formation of the solar system) evolution of the Galaxy, Rood et al. (1976) found that the interstellar abundance of ${}^3\text{He}$ should have doubled in the last 4.5 Gyr. Although this prediction is not in conflict with much of the recent data obtained by Rood et al. (1984), their result that ${}^3\text{He}/\text{H} (\text{W3}) \approx 10\text{--}20({}^3\text{He}/\text{H})_{\odot}$ appears anomalous.

The present observational and evolutionary uncertainties appear too large to decide if primordial production of ${}^3\text{He}$ is *required*. It is, however, possible to set an *upper* limit to the primordial abundance of deuterium and helium-3 by the requirement that D and ${}^3\text{He}$ not be *overabundant* at the time of formation of the solar system (YTSSO). For example, suppose that the nucleon abundance η is small, so that large abundances of D and ${}^3\text{He}$

are produced primordially (see Figure 2 and Table 1). By the time of the formation of the solar system, any “excess” D must have been burned away by having been cycled through stars. But D is burned to ^3He in stars, and some of the ^3He in the cooler, outer layers will survive and be returned to the interstellar medium. Therefore, some of the “excess” deuterium reappears as ^3He , and care must be taken that “too much” ^3He is not produced in this manner. As YTSSO show, the solar system abundances of D and ^3He provide an upper limit to the sum of the primordial abundances of D *plus* ^3He :

$$[(\text{D} + ^3\text{He})/\text{H}]_{\text{p}} < (\text{D} + ^3\text{He})_{\odot} + (g_3^{-1} - 1)(^3\text{He}/\text{H})_{\odot}. \quad 19.$$

In Equation 19, g_3 is the fraction of ^3He that survives stellar processing; YTSSO suggest that $g_3 > 1/4$, while Truran & Brunish (1985) estimate that $g_3 > 1/2$. For $[(\text{D} + ^3\text{He})/\text{H}]_{\odot} < 4.2 \times 10^{-5}$, $(^3\text{He}/\text{H})_{\odot} < 1.8 \times 10^{-5}$ (see Equation 18), and $g_3 > 1/4$ – $1/2$, we find that $[(\text{D} + ^3\text{He})/\text{H}]_{\text{p}} < 6.0$ – 9.6×10^{-5} , so that (see Table 1) $\eta_{10} > 3$ – 4 (YTSSO). This approach to the primordial abundances using the solar system data has the advantage of being relatively independent of the model of galactic evolution.

3.4 Helium-4

It is clear from Figure 2 that the primordial ^4He abundance must be known to an unprecedentedly high accuracy to provide constraints on the parameters of the Big Bang. The abundance of ^4He has been determined in a number of astrophysical sources: the atmospheres of young stars, the atmospheres of old stars, planetary nebulae, gaseous nebulae (H II regions) in our Galaxy and in other galaxies, and the isolated extragalactic H II complexes. Various model-dependent estimates have been made for the Sun, the solar system, and globular clusters. The amazing constancy of the ^4He abundance (to $\pm 20\%$) in these various objects points to a uniform origin: synthesis during the Big Bang. To reveal the physical conditions at that epoch, however, the abundance must be known to better than $\pm 5\%$. Furthermore, because of the general enrichment in ^4He during stellar and galactic evolution, observations of unprocessed material are needed; otherwise, models of the enrichment including the initial mass function, stellar mass loss processes and quantities, stellar evolution and internal structure and mixing, etc., are needed to deduce the pregalactic abundance.

Since the nuclear reaction rates for ^4He production are known to within a few percent, the predictions of the standard model are well established. With a well-known pregalactic ^4He abundance, other parameters besides the nucleon-to-photon ratio can be discerned, such as the number of neutrino types. The best determinations of primordial ^4He come from observations of the emission-line spectra of gaseous nebulae. Therefore, we

concentrate on these and discuss other methods and results briefly. A recent ESO workshop on "Primordial Helium" (Shaver et al. 1983a) contains many excellent papers on all aspects of both the observations and the theoretical background.

3.4.1 GASEOUS NEBULAE A number of authors have described the problems associated with the observations and interpretations of the H II emission spectra; see Stasinska (1983) and Davidson & Kinman (1985) for recent discussions. The recombination emission lines of H I, He I, and He II are observed and compared with the relative emissivities predicted by recombination theory; these predicted line strengths are well known and are not sensitive to the electron temperature and electron density that characterize the H II region. Observational constraints result from the range in line strengths, since the H I Balmer lines are much stronger than the He I lines. Either a linear detector with a large dynamic range is needed, or else special care must be taken with calibration through intermediate-strength features. Another constraint concerns the angular dimension of the H II region. The extragalactic H II regions, which have a more nearly primordial composition, have a smaller angular size, and thus the projected spectrographic slit covers an array of physical characteristics (especially ionization conditions) such that the slit includes an admixture of multiple He^0 and He^+ zones. In contrast, the nearby galactic H II regions, which can be more selectively sampled, contain extra He due to stellar processing. Since the chemical history of the galactic H II regions cannot readily be determined, most investigators have searched for isolated H II regions with unprocessed, low metal content matter to determine the primordial He value Y_p (e.g. Searle & Sargent 1972, French 1980, Tully et al. 1981, Kunth & Sargent 1983, Davidson & Kinman 1985).

Recombination theory predicts line strengths that are reasonably independent of electron temperature and density. However, complications result from the specific physical conditions. For example, (a) the observed line intensities may have to be corrected for underlying stellar H I and He I and II absorption features. (b) Corrections for interstellar reddening need to be applied; these may be complicated by a nonstandard distribution of dust or nonstandard-sized dust grains (see Tully et al. 1981, for example). (c) The correction for (unobservable) neutral He can be substantial. (d) If there are spatial temperature fluctuations, the physical parameters and derived abundances will be affected (e.g. Peimbert 1971, Lequeux et al. 1979). (e) For the helium lines, the influence of self-absorption and resonance fluorescence should be assessed (Robbins 1968).

The O abundance is generally taken as an indicator of the amount of stellar processing that has occurred in a given H II region. The forbidden

lines in a nebula provide the cooling, and lines of [O II] and [O III] are present even when the O abundance is low. Furthermore, the ratio of the [O III] intensities of $\lambda 5007$ and $\lambda 4959$ to $\lambda 4363$ provides the most convenient measure of the electron temperature, while the relative strengths of the [O II] doublet $\lambda 3726, \lambda 3729$ and of the [S II] doublet $\lambda 6717, \lambda 6731$ are sensitive to the electron density (see Osterbrock 1974, Pradhan 1978). Ionization correction factors derived from observations of [O I], [O II], and [O III] lines are often used to estimate the corrections to be applied to observed ionic abundances for neutral He to derive the total abundance of He and of other elements as well. Often He II $\lambda 4686$ can be observed and provides a determination for He^{++} . Unfortunately, the helium ionization correction factor appears to be correlated with the O abundance [e.g. see Tables 6 and 9 from Peimbert & Torres-Peimbert (1977) for the Orion Nebula].

There are many subtle and not-so-subtle effects that influence the final abundances. These are well discussed by Davidson & Kinman (1985), but they have also been assessed by other workers, e.g. Peimbert & Torres-Peimbert (1974), Lequeux et al. (1979), French (1980), Kunth & Sargent (1983).

A primordial He abundance might be deduced from galactic H II regions either from observations where the metallicity is very low or from a variation in He with metallicity and galactocentric distance. Helium abundances $N(\text{He})/N(\text{H})$ have been determined for galactic H II regions from optical spectra by Peimbert & Costero (1969), Peimbert & Torres-Peimbert (1977), Peimbert et al. (1978), Hawley (1978), Talent & Dufour (1979), and French (1981). The average $^4\text{He}/\text{H}$ abundance is 0.113 ($Y = 0.305$ with $Z = 0.02$) as shown by Shaver (1983), with considerable scatter and no gradient with galactocentric distance. The optical data on $N(\text{He}^+)/N(\text{H}^+)$ have been supplemented by radio measurements of $N(\text{He}^+)/N(\text{H}^+)$ by Shaver et al. (1983b) to look for a gradient by using a larger range in galactic distance. There is no evidence for a gradient in that sample either, although the complications introduced by metallicity variations and by looking at the ionic ratio only are difficult to quantify. Since the observations are not concentrated toward the top of the distribution in $N(\text{He}^+)/N(\text{H}^+)$, it is clear that there is a large variation among H II regions in the amount of neutral He and that an important fraction of the He is neutral. This point, which can be examined in more detail in the nearby H II regions of the Galaxy, is important for the extragalactic H II regions too. While local H II regions give us many insights into the physics of these regions, they are not well suited for determining primordial He because the material is too processed and the correction for neutral He is high and uncertain.

The best objects are the blue compact galaxies or extragalactic H II

regions, which might better be called “intergalactic” H II regions because they are individual, primarily gaseous, unevolved complexes. Zwicky (1966, 1971) has described the blue compact galaxies, and attention has been called to them by Sargent & Searle (1970). These objects, which have been studied by many researchers such as Searle & Sargent (1972), Lequeux et al. (1979), French (1980), and Kunth & Sargent (1983), are characterized by high H mass to total mass, low total mass, and low O abundance, all of which imply little processing of gas into stars and little stellar evolution.

The approach of Lequeux et al. (1979), based on an idea of Peimbert & Torres-Peimbert (1974), was to examine He vs. O abundances and extrapolate back to zero O (i.e. zero metallicity). From their study of eight irregular and blue compact galaxies and both Magellanic Clouds, Lequeux et al. derive a value for Y_p of 0.228 ± 0.014 (3σ error). However, the range in Y at fixed Z is large. For example, II Zw 70, IC 10-1, and II Zw 40 all have $Z \approx 0.004$, but Y varies from 0.23 to 0.25. In contrast, IC 10-2 with $Z \approx 0.0075$ and the Small Magellanic Cloud (SMC) with $Z \approx 0.0026$ have virtually identical ^4He abundances. It is worth noting that for the five H II regions with the lowest metal abundance ($Z < 0.004$), we have $\langle Y \rangle = 0.238$.

French (1980) studied chemical abundances in ten low-luminosity galaxies with spectra like giant H II regions and in four high-luminosity objects. He combined his results with those published for six other objects (including the Magellanic Clouds) and found a relationship between He/H and O/H similar to that of Lequeux et al. (1979) with considerable scatter; his result is heavily influenced by the very low He/H measured in I Zw 18, however, which he later suggests was in error because of contamination by the night sky (private communication to GS, 1981). Rosa (1983) presents evidence for a He gradient (and O/H gradient) in H II regions in M101; his value for Y_p is 0.24.

However, Kunth & Sargent (1983) found no correlation between He and O in their sample of 12 metal-poor low-luminosity galaxies, although the limited range in Z of their sample would have precluded detection of such a correlation. To find metal-poor objects, they selected complexes of high electron temperature; these would be expected to be hot because of the lack of the metals necessary for cooling. They should also lack neutral He. Kunth & Sargent did a careful analysis and assessment of errors, and they found a weighted mean helium abundance from those 12 galaxies to be $Y_p = 0.245 \pm 0.003$. They then combined results from Lequeux et al. (1979), French (1980), and Kinman & Davidson (1981) (after correcting Kinman & Davidson's He^+ plus He^{++} results for neutral He) with their own and a few others and found $Y_p = 0.247 \pm 0.007$. These results are shown in Figure 9, taken from Kunth (1983). While the results do not exclude the possibility of

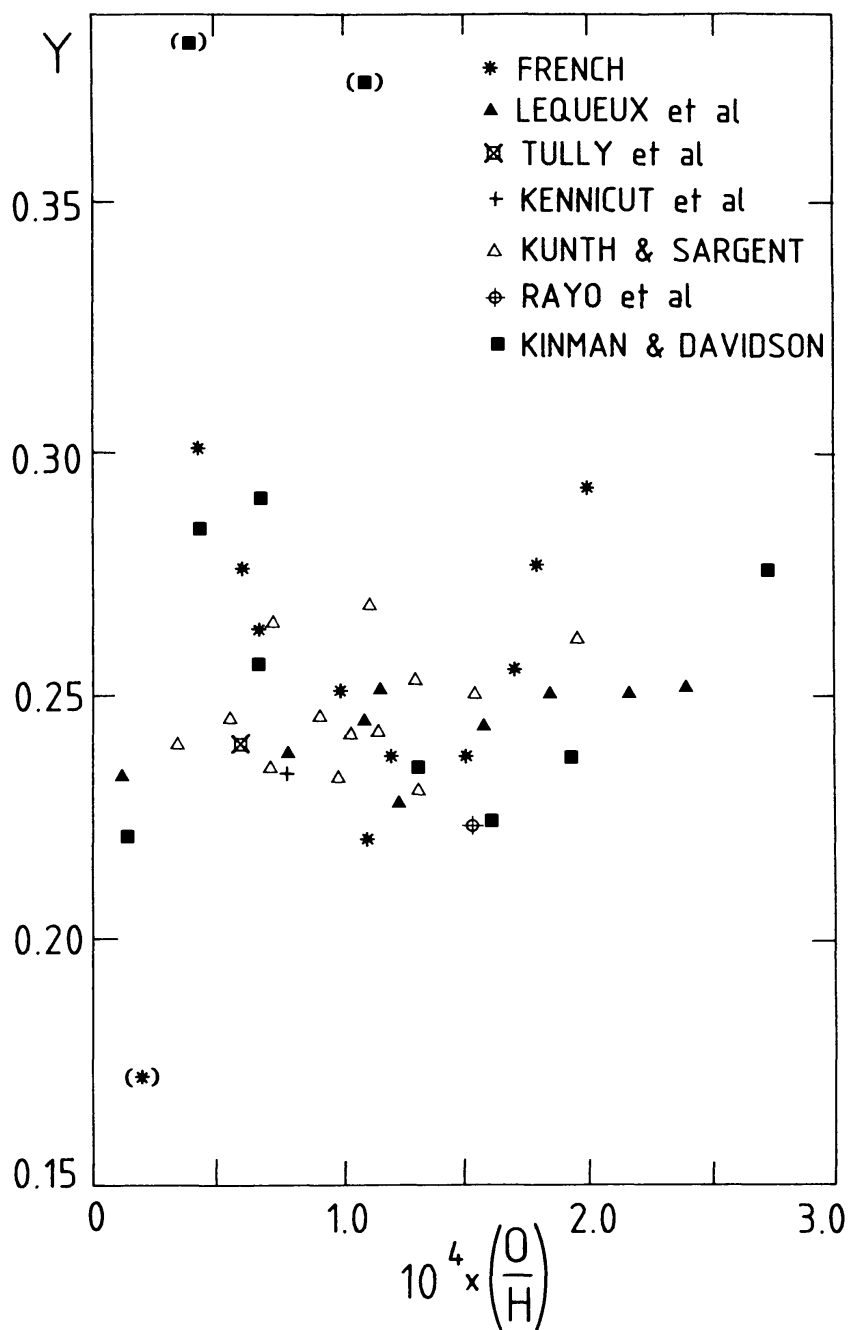


Figure 9 A compilation of determinations of Y from measurements in metal-poor low-luminosity objects versus the O/H determination. (For comparison, the solar O/H value is 8.3×10^{-4} .) (From Kunth 1983.)

a variation of Y with metallicity Z at higher Z values, they do show that for metal-poor systems there is no discernible trend beyond the error bars. Thus the mean Y value is a better estimate of primordial He than that extrapolated through large scatter to zero O/H.

The final best value given by Kunth & Sargent (1983) from the metal-poor galaxies alone is

$$Y_p = 0.245 \pm 0.003.$$

Another approach is to use individual well-measured objects, preferably of low metallicity. This approach has been taken by Rayo et al. (1982), who found a pregalactic Y_p value of 0.216 for an H II region in M101 from the Y vs. Z extrapolation. A similar value is given by French & Miller (1981) from their study of NGC 4861; however, they ignore the correction for neutral He and attach no uncertainty to their determination. Recently, Davidson & Kinman (1985) have done such a study of the metal-poor object I Zw 18, with special care and attention paid to all the sources of error. It is instructive for workers in this field to read and heed their cautions. They express their result in terms of an equation, stating that "it is easily possible—but not yet proven!—that $Y \approx 0.24$," with Y_p only slightly (-0.003) smaller.

The issues of Y vs. Z , the larger scatter in the He vs. O values, and the individual low values found for He/H are discussed further by Kunth (1983) and by YTSSO. It seems clear that additional work will be done to determine Y_p more precisely in the future; it is as important to cosmological studies as the determination of H_0 .

3.4.2 PLANETARY NEBULAE Most of the specific means of chemical analysis and sources of error for gaseous nebulae discussed in the previous section apply to the planetary nebulae (PNs). There are two greater difficulties in deducing Y_p from them, however: the contamination due to general galactic chemical enrichment, and the contamination due to the processing by the central star of the given PN itself. The former can be neglected only for the halo population PNs. An excellent review on He in PNs has been presented by Peimbert (1983).

Type I PNs are He rich, with stars more massive than $2.4 M_\odot$ as their progenitors (Peimbert & Serrano 1980). They will be strongly affected by both galactic and stellar chemical evolution and are therefore not good sites to determine Y_p . The disk planetaries, types II and III, have progenitors with masses of 1.4 – $1.5 M_\odot$ (Alloin et al. 1976). With guidance from stellar evolution theory (e.g. Renzini & Voli 1981), we can estimate the changes in the stellar surface composition and then the stellar enrichment factor. Peimbert (1983) has derived a value of $Y_p = 0.227$ for six disk PNs primarily

from Torres-Peimbert & Peimbert (1977) and a value of $Y_p = 0.220$ for the larger sample (16) of Peimbert & Serrano (1980). A major source of uncertainty is the assumption about galactic enrichment: that the change in He abundance is three times the change in metallicity. Barker (1978) points out that incomplete ionization of He also affects the He abundance in PNs.

For the halo PNs, He production due to galactic evolution is neglected, and stellar production is determined from theory. Peimbert's (1983) compilation of parameters for the three best-observed halo PNs results in $Y_p = 0.218$.

In spite of the good agreement in Y_p among the various planetaries, the results are very model dependent and rest on many assumptions about stellar and galactic evolution. There are also the additional problems common to both the observations and the analysis of gaseous nebulae.

3.4.3 GLOBULAR CLUSTERS The globular clusters are known to be old and metal poor and therefore can be expected to contain the primordial He abundance. There are several features of their color-magnitude diagrams that are sensitive to the He content: the blue edge of the instability strip, the width of the instability strip, the luminosity of the main-sequence turn-off point, the luminosity of the horizontal branch, the ratio of the number (or theoretical lifetime) of horizontal branch (HB) stars to red giant (RG) branch stars, etc.

A historical overview was presented by Caputo & Castellani (1983). Cole et al. (1983) have discussed the various methods to find the He content in globular clusters and conclude that the most productive avenue is likely to be through main-sequence stars, since they have not suffered the internal mixing as have the evolved stars. This applies to both the cluster dwarfs and the field subdwarfs. Carney's (1983) results for the halo field stars give $Y_p = 0.19$, but he, Cole et al. (1983), and Perrin (1983) all point out that more accurate parallaxes would improve the He determination.

Since the luminosities of the HB and of the main-sequence turn-off depend on the He content, but in opposite senses, a comparison of the two luminosities is potentially a powerful way to find Y_p (Caputo & Cayrel de Strobel 1981, Vandenberg 1983). Cannon (1983) has recently reviewed the status of the observations and the theory on this matter. Improvements in both the theoretical and observational aspects are currently being made by a number of researchers.

The comparison of theoretical lifetimes of HB stars to RG stars (or more precisely the ratio of the number of HB to RG stars), first suggested by Iben (1968), has been applied to derive the He content in these evolved stars. The value of Y so deduced by Buzzoni et al. (1983) from a specific subset of clusters is 0.23 ± 0.02 .

For all the methods of determining Y_p from globular clusters, there are large uncertainties and systematic errors in the fitting of cluster diagrams to theory and in estimating effects due to age, metallicity, internal mixing, etc. Since there is much current interest in globular cluster research, we are optimistic that better estimates of Y_p will be forthcoming.

3.4.4 STELLAR ATMOSPHERES Unfortunately, the spectral lines of He I and He II are not present in the photospheres of most stars. They can be found only in hot O and B stars. These are the youngest, most recently formed stars, so their He content has been modified by generations of previous stars. The present-day He abundance in these stars can be found through comparison of theoretical line profiles with observed ones. The theoretical computations of Auer & Mihalas (1973) take into account effects due to non-local thermodynamic equilibrium (non-LTE), and reasonable agreement was found in the comparison with the observed line profiles in four B stars by Mihalas et al. (1974, 1975). More recently, Heasley et al. (1982) and Wolff & Heasley (1985) have observed many B stars with modern detectors and have made detailed comparisons with observed and computed profiles of Auer & Mihalas for several of the He lines. The non-LTE effects are still not completely corrected for in some of the lines, so that while relative He abundances can be found, absolute abundances at the precision needed for cosmology have not been obtained. Nissen (1983) has reported line profile comparisons for the He I 4026 line, where non-LTE effects are negligible, with high-resolution observations; he finds that Y (not Y_p) = 0.28 ± 0.04 .

Most stellar He abundances have been based on equivalent widths rather than line profiles. Norris (1971), for example, finds that $Y = 0.28$. Halo OB stars have been studied by Keenan et al. (1982), who find that $Y = 0.28$ and suspect that their stars are Pop I escapees from the galactic disk.

Nissen (1974, 1976) has studied He abundances in B stars in young clusters and associations by means of narrow-band filter photometry, which measures the He I 4026 line intensity. The system can be calibrated on standard stars, and high-accuracy photometric measurements can be obtained. Whereas most of the cluster stars appear to have $Y = 0.28$, some clusters (e.g. η and χ Per, Cep OB III) show dramatically different results with $Y = 0.19$. Wolff & Heasley (1985) have calibrated and verified Nissen's results through high-resolution spectroscopy.

Differential He abundances can also be determined for F stars from their positions in the Strömgren $c_1, (b - y)$ diagram, as discussed by Strömgren et al. (1982). They find significant differences in the position of the main sequences between the Hyades and Coma clusters, probably due to He abundance differences. Nissen (1983) shows results for two other clusters, one similar to the Hyades, the other like field stars. Effects such as rotation

and CNO abundance may contribute to the difference in main-sequence position.

The value for He from young O and B stars is near $Y = 0.28$. However, there is interesting evidence from the work on young cluster stars that the amount of galactic He enrichment varies with position. Therefore the step from present-day He abundance to primordial contains considerable uncertainty, and a warning should be heeded even for shorter steps back to primordial He.

3.4.5 SOLAR SYSTEM A protosolar He abundance can be estimated from meteorites. Anders & Ebihara (1982) give $Y = 0.24$. The solar system abundance from the giant planets might be expected to be that of the primitive solar nebula, since neither H nor He would condense, but some differentiation may have taken place during subsequent evolution. Voyager results from Jupiter have been reported by Gautier et al. (1981), who find Y between 0.17 and 0.24. Some differentiation has taken place in Saturn, where $Y = 0.135 \pm 0.045$ was given by Conrath et al. (1982) according to Gautier (1983). These values, only presolar, are too uncertain for cosmological purposes.

The solar He abundance cannot be found from photospheric absorption lines and must be inferred by other means. Heasley & Milkey (1978) found $y = 0.10 \pm 0.025$, which corresponds to $Y = 0.28 \pm 0.05$ (with $Z = 0.02$) from solar prominences, but they note the large (and realistic) error bars. Solar models can be used to find He from the luminosity and radius with an assumption about the metallicity. Bahcall et al. (1982) use 0.023 for the metallicity-to-hydrogen ratio (Z/X) at $t = 0$ and deduce that $Y = 0.25 \pm 0.01$ (3σ error). Solar oscillations (Grec et al. 1980, 1983) are also indicative of the Sun's internal structure and its He content. Christensen-Dalsgaard & Gough (1980) and Gough (1983) give a value for the present solar He abundance of 0.25 ± 0.02 .

From the solar, planetary, and meteoritic results, the present solar system He value is probably about 0.26 ± 0.03 , which is an upper limit to the primordial value.

3.4.6 SUMMARY At the present, the best value for Y_p comes from the isolated extragalactic H II regions, which show little stellar processing. It is likely that there is a change with time in the relative enrichment of He vs. the metals, but at low metallicity there is sufficient scatter in the determinations of He/H as a result of the many uncertainties that the trend with metallicity is not readily discernible. It thus appears safest to adopt the approach of Kunth & Sargent (1983), who find Y_p from the observed average Y (with no extrapolation to $Z = 0$) from metal-poor emission-line galaxies. Combined

results for low-metal H II regions from various workers are given by Kunth (1983):

$$Y_p = 0.245 \pm 0.003.$$

The unevolved halo stars, both globular cluster main-sequence stars and field subdwarfs, are another potential source for Y_p . Their values require accurate fundamental stellar data, such as parallax, and/or good stellar models, but do not require knowledge of the stellar and galactic enrichment of He. Other stellar and nebular results (including the planetaries) demand detailed understanding of stellar processing of He and galactic chemical evolution. The variation in the values of the He content in the young Pop I stars reveals the difficulties in trying to assess the amount of processing.

3.5 *Lithium*

Abundances of Li have been determined in hundreds of stars in various stages of stellar evolution. All of the abundances are based on measurements of the equivalent width of the Li I resonance doublet at 6707.761 and 6707.912 Å. The absolute gf -values for these transitions are well known: Wiese et al. (1966) give 1.0 and 0.50, respectively, virtually the same as the modern measurements that include the hyperfine splitting of Gaupp et al. (1982) (0.989 and 0.494). The ^6Li doublet is shifted by 0.16 Å to the red from the ^7Li wavelengths above.

As a star evolves, its surface Li is subject to destruction and dilution. The transport of Li through convection, convective overshoot, gravitational settling, turbulent diffusion, rotationally induced meridional circulation, etc., to interior regions will destroy Li at temperatures hot enough for (p, α) reactions ($T = 2 \times 10^6$ K); in addition, the surface Li will be diluted through mixing of the outer layers containing Li with the interior regions where Li has been destroyed previously. Therefore, the best place to find the primordial Li is in stars that are young enough to have undergone little evolution or massive enough not to have spent much time on the pre-main-sequence convective track. Further restrictions on what stars can be studied for Li result from the atomic structure of Li: The single-valence electron of Li I and consequent low ionization potential mean that the resonance line of Li I is too weak to observe in stars hotter than about 8000 K, while He-like Li II, the dominant ion, has its resonance line at 199 Å. [Because of the low abundance of Li, most observations have been made of the Li I resonance doublet, although a subordinant line at 6104 Å has been measured in sunspots and in Li-rich red giants (e.g. Merchant 1967, Wallerstein & Sneden 1982, Lambert & Sawyer 1984).]

3.5.1 POPULATION I The maximum values of Li/H found in T Tauri stars and other pre-main-sequence stars, in stars in young galactic clusters, in

meteorites, and in the interstellar gas have been thought to represent the “initial” abundance of Li. Zappala (1972) summarized his and others’ relevant results for Li/H that are thought to be the original Li abundance that the star inherited at birth. His value for Li/H was 10^{-9} for young T Tauri stars and pre-main-sequence stars in NGC 2264. He also showed that the observed maximum Li/H in the Hyades, Praesepe, and Pleiades stars is 10^{-9} ; it was clear that the extrapolation of Li/H vs. effective temperature for main-sequence stars toward hotter temperatures, i.e. higher masses, would not go above 10^{-9} . New detectors for high-resolution spectroscopy have brought more and fainter cluster stars within reach for higher-accuracy determinations. Recent work on the F and G stars in the Pleiades (Duncan & Jones 1983) and the Hyades (Cayrel et al. 1984, Duncan & Jones 1983) confirm the maximum Li/H value of 10^{-9} . The field stars give the same result. Duncan’s (1981) observations of Li I in F5–G5 dwarfs show that the hottest and, as he promotes, the youngest stars have that same value. A recent complementary study by Boesgaard & Tripicco (1985) of F0–F5 field dwarfs also shows that these stars share the same upper value, although many of the field stars have depletions of factors of 4–200. The Sun is one of the main-sequence stars with a large Li depletion; Muller et al. (1975) found $(\text{Li}/\text{H})_{\odot} = 10^{-11}$ for a depletion factor of 100 relative to the Pop I maximum value. The meteoritic value of Li/H [= (Li/Si)(Si/H) = 2.6×10^{-9} (Nichiporuk & Moore 1974, Cameron 1982, Lambert & Luck 1978)] is a more appropriate pre-solar-system value.

Figure 10 shows the Pop I Li/H values for the Hyades, Pleiades, and field stars. Note the uniformity of the upper bound in this figure. As discussed by Herbig & Wolff (1966), the destruction of Li is a function of both mass and age during pre-main-sequence and main-sequence evolution. These effects can be seen in Figure 10: For the clusters the stars are close to the same age, so the influence of the differing masses can be seen, while the field stars show an array of ages, which presumably accounts for the range in Li depletion. [Duncan & Jones (1983) suggest, however, that the range in Li at a given spectral type in the Pleiades is due to a spread in time of formation of the stars in that cluster. Some of the range could be attributable to possible short-term temporal variability in the Li I line strength in a given star due to variable chromospheric activity in young solar-type stars, as implied by Giampapa’s (1984) solar observations.]

Although the observations show that there are many field stars that contain less Li than the maximum value, the details of the nature of the circulation that results in the depletion are not well understood. Bodenheimer (1966) has calculated the pre-main-sequence convective destruction of Li, and his results match the Duncan & Jones (1983) Pleiades results fairly well. (With different input conditions and a mixing length to

scale height ratio of 2 to characterize convection, Mazzitelli & Moretti (1980) claim greater pre-main-sequence depletion, however.) Since the Hyades relative to the Pleiades show more depletion at a given mass for the cooler stars, it is apparent that there is additional destruction on the main sequence; this phenomenon apparently is observed in the case of the field stars too. Two major mechanisms have been proposed and described in some detail: turbulent and microscopic diffusion (Vauclair et al. 1978), and convective overshooting (Straus et al. 1976). At a given mass the amount of Li depletion is primarily a function of the main-sequence age of the star, such that the oldest stars have had time to destroy more of their Li than the newly arrived main-sequence stars (e.g. see Duncan 1981).

All the recent cluster observations of F and G stars in the Pleiades, the Hyades, and the field confirm that the maximum Li/H value is uniform and comparable to that in the interstellar gas. The key observations of the young interstellar gas clouds have to be made with sensitive detectors

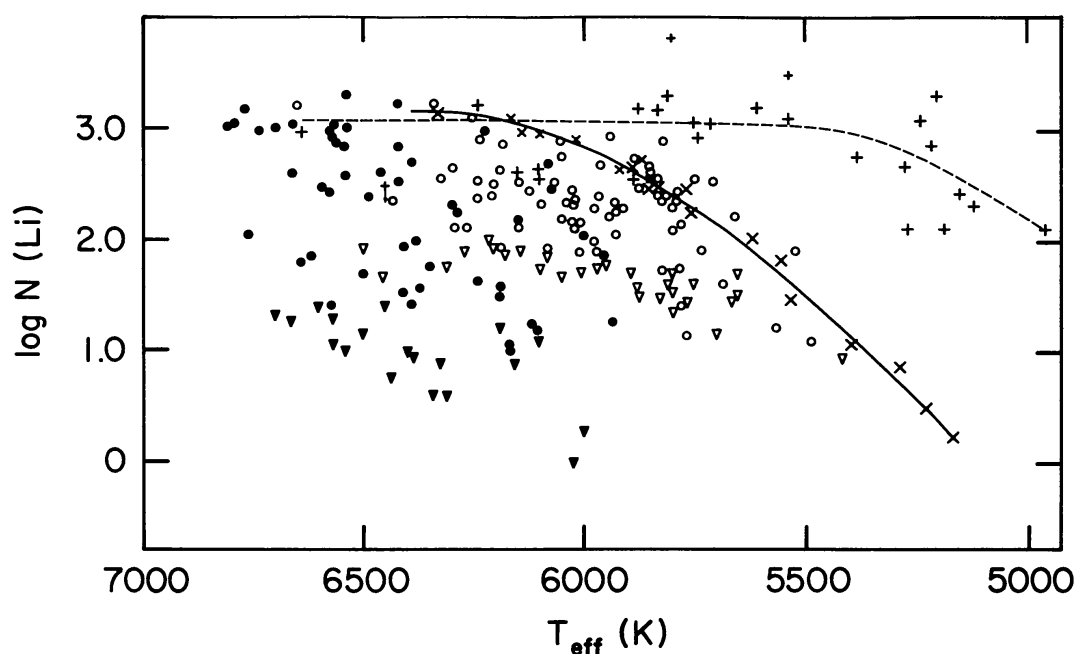


Figure 10 Lithium abundances in Pop I stars plotted [on the scale where $\log N(\text{H}) = 12.00$] as a function of stellar effective temperature. The solid circles are from the survey of F0–F5 field dwarfs of Boesgaard & Tripicco (1985), and the open circles are Duncan's (1981) survey of F5–G5 field dwarfs; open and filled triangles represent upper limits from the respective surveys. The crosses (\times) are from the Hyades results of Cayrel et al. (1984) (large crosses) and Zappala (1972) (small crosses), the latter as reanalyzed by Duncan & Jones (1983). The solid line shows the curve of Li depletion with stellar mass for the Hyades. The plus symbols are for the Pleiades dwarfs from Duncan & Jones (1983), with the larger symbols representing higher-quality data. The dashed line is an uncertain curve of Li depletion with stellar mass for the Pleiades. Large depletions of Li can be seen, but the maximum is uniform over a temperature range of 1500 K.

because the Li I resonance line is very weak. In fact, the first detection by Traub & Carleton (1973) was along the line of sight to ζ Oph, where the Li I equivalent width was 0.68 mÅ. The largest line strengths have been found toward 55 Cyg and ρ Oph A and are 3–5 mÅ (Vanden Bout & Grupsmith 1974, Hobbs 1984). Other detections and abundance ratios have been reported by Vanden Bout et al. (1978), Snell & Vanden Bout (1981), Hobbs (1984), and Ferlet & Dennefeld (1984). However, the Li/H values derived from these measurements and the assumptions about the physical conditions in the gas result in numbers for Li/H not far below 10^{-9} , except for ζ Oph and δ Sco, where Li seems clearly to be depleted (Ferlet & Dennefeld 1984). However, since most of the interstellar Li will be in the form of Li II, while it is Li I that is observed, these analyses must make (uncertain) assumptions about the ionization field to derive Li/H abundances.

Post-main-sequence stars are expected to show some Li dilution as the surface convection zone deepens. There is a remarkable coincidence of the theory with the observed (diluted) values when $\text{Li}/\text{H} = 10^{-9}$ is taken as the main-sequence abundance for the $M \geq 1.3 M_{\odot}$ progenitor stars (Boesgaard 1971, Alschuler 1975, Boesgaard et al. 1977, Lambert et al. 1980). For an informative discussion of the composition changes found in G and K giants, see Lambert et al. (1980). This picture has recently been demonstrated to be more complex by the observations of Pilachowski et al. (1984) of Li in the giant branch of the old galactic cluster NGC 7789; in particular, some of these stars show the same maximum Li value as that of unevolved F stars, which Pilachowski et al. suggest may indicate that the original Li was not depleted on the subgiant or giant branches. The study of Li in the weak G-band giants of Lambert & Sawyer (1984) confirms that Li in these stars is overabundant relative to normal G and K giants, but that it does not exceed the “cosmic” value of $\text{Li}/\text{H} = 10^{-9}$. They argue that Li was preserved via upward diffusion while the stars were upper main-sequence chemically peculiar stars. As they point out, any production mechanisms in evolved stars cannot be guaranteed to achieve the “cosmic” Li value and yet not overproduce Li in some instances. The “super-Li-rich” stars are rare, but the S star, T Sgr (Boesgaard 1970), and some carbon stars (Torres-Peimbert & Wallerstein 1966) appear to have one or two orders of magnitude more Li (as measured by Li/Ca or Li/Na ratios) in their atmospheres than young, unevolved stars (Boesgaard 1976).

The maximum Li/H value from the time of the origin of the solar system (as measured in meteorites) to the present (as found in the youngest stars and the interstellar gas) seems to have remained remarkably constant. A summary is presented in Table 2. The net effect of Li destruction and Li production in the galactic disk on the overall Li abundance thus appears to have been small.

3.5.2 POPULATION II Recently, Li I has been discovered in several halo dwarfs by Spite & Spite (1982a,b). They argue persuasively that their derived abundance represents primordial Li. Further work by Spite et al. (1984) doubles the sample of halo stars to 25 and confirms the earlier results. Figure 11 shows the combined Li results from the two papers plotted as a function of the effective temperatures that they have used.

The mean Li/H for the 17 stars between 5500 and 6300 K is $1.12(\pm 0.05) \times 10^{-10}$, although Spite et al. (1984) suggest that the true error exceeds that of the formal mean and take $\text{Li/H} = 0.7\text{--}1.8 \times 10^{-10}$. Spite & Spite (1982b) and Spite et al. (1984) review various mechanisms of Li depletion and rule them out: (a) The metal deficiency should result in a shallower, not deeper, convection zone; (b) the stars are slow rotators, so meridional circulation will not play a strong role; and (c) mass loss by stellar winds ought to result in a mass-dependent Li depletion. Recent calculations on pre-main-sequence depletion (D’Antona & Mazzitelli 1984) show effects only for the coolest stars, while those calculations of main-sequence diffusion (Michaud et al. 1984) cannot reproduce the observed lack of dependence of Li abundance on stellar mass. Note that the observed mass range is very small, however. The case against any Li depletion in these stars is partly qualitative and argued by analogy. It seems clear from the halo dwarf results that *some* Li was present at the time of the halo formation.

Meneguzzi et al. (1971) showed that galactic cosmic rays (GCRs) could produce the isotopes of Li, Be, and B via spallation reactions on C, N, and O nuclei in the interstellar gas. [See Reeves (1974) for a review of the origin of the light elements.] The observed light element ratios indicated that GCR reactions produce about 2×10^{-10} for Li/H, of which about 30% is ^6Li , and about 2×10^{-11} for Be/H. Maurice et al. (1984) found no evidence for ^6Li in halo stars, while Molaro & Beckman (1984) could not detect Be in the

Table 2 Population I “initial lithium” (after Zappala 1972)

Object	Li/H	References
FU Ori	10^{-9}	Zappala (1972)
T Tauri stars	5×10^{-10}	Zappala (1972)
NGC 2264	10^{-9}	Zappala (1972)
Pleiades (max)	9×10^{-10}	Zappala (1972), Duncan & Jones (1983)
Hyades (max)	8×10^{-10}	Zappala (1972), Duncan & Jones (1983)
Chondrites, Type I	2.6×10^{-9}	Nichiporuk & Moore (1974)
Young field stars (max)	10^{-9}	Boesgaard & Tripicco (1985)
Interstellar gas	$\lesssim 10^{-9}$	e.g. Hobbs (1984)

halo dwarf they observed with IUE. These results imply that the Pop II Li is not contaminated by GCR-produced ^7Li or ^6Li .

Some of these stars in Figure 11 do show some depletion also; they are plotted as upper limits. For the cooler stars, this is attributed to pre-main-sequence convective depletion and appears consistent with calculations by D'Antona & Mazzitelli (1984). For stars of the same temperature (mass), there is a range in the observed Li I line strength and in Li/H of a factor of 2 at $T = 5800$ K; presumably this indicates that there is some depletion.

As is customarily argued for ^4He , the near-universality of the $^7\text{Li}/\text{H}$ ratio implies a universal origin for ^7Li .

3.5.3 POPULATION I VS. POPULATION II Universality arguments can be applied to both the Pop I (10^{-9}) and the Pop II (10^{-10}) Li/H contents. Either the Pop II abundance represents the primordial Li and the galactic disk has enriched itself in Li uniformly by a factor of 10, or else the Pop I star

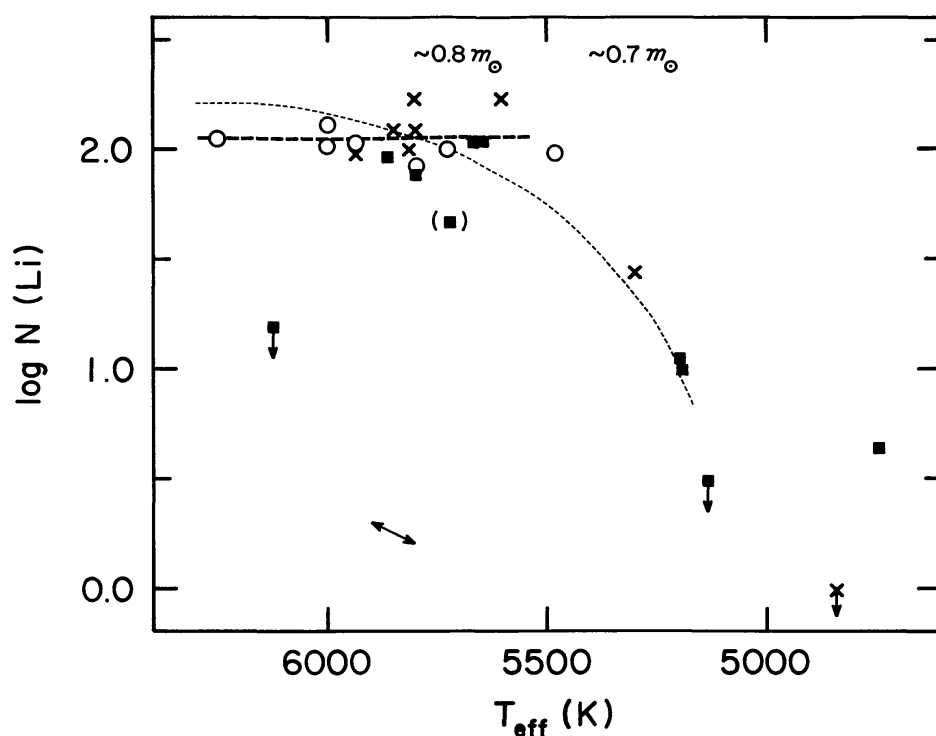


Figure 11 Lithium abundances in Pop II stars [with $\log N(\text{H}) = 12.00$] as a function of stellar effective temperature. The different symbols represent different $[\text{Fe}/\text{H}]$ abundances: open circles ≤ -2.0 ; crosses -1.5 to -2.0 ; filled squares ≥ -1.5 . The horizontal dashed line is the mean of the upper points. Arrows on the points indicate upper limits. The square in parentheses is an uncertain determination caused by a cosmic-ray event near the Li line. The light dashed curve shows the pre-main-sequence Li depletion calculated by D'Antona & Mazzitelli (1984) for an initial value of $\log \text{Li} = 2.2$. The arrow in the lower left shows the effect of a temperature change of 100 K on the derived Li abundance. (After Spite et al. 1984.)

maximum represents the original amount of pregalactic Li and the Pop II stars have uniformly destroyed Li by a factor of 10.

If the first hypothesis is correct, what evidence is there for Li production in the disk and what explains the factor of 2.2 in the Li content at the same stellar mass in Pop II stars? Lithium has long been thought to be produced in spallation reactions of galactic cosmic rays on C, N, and O atoms in the interstellar gas (Meneguzzi et al. 1971). However, to be consistent with the abundance of Be and B, this source can only produce a Li/H content of $\sim 2 \times 10^{-10}$, for a total Pop I amount of 3×10^{-10} . Among the sources of Li mentioned in Section 3.1, production in red giants and in novae seems the most plausible (Audouze et al. 1983). But the constancy of the maximum, at least over the last 5×10^9 yr, requires that the interstellar gas be well mixed so that all Pop I stars have the same initial Li. The only direct evidence for Li production comes from the few Li-enriched red giants—S and C stars [see Boesgaard (1976) for a summary]. Wallerstein & Sneden (1982) have found a Li-rich, ^{13}C -enhanced K giant and discuss the production of Li in this evolved star. Lithium may be somewhat depleted in Pop II stars of the same mass because of differences in characteristics like rotation and meridional circulation.

If the second hypothesis is correct, what explanation might there be for the destruction of Li so uniformly in the Pop II stars? Many theories have been advanced for the Li destruction in Pop I F and G dwarfs (e.g. Bodenheimer 1966, Straus et al. 1976, Vauclair et al. 1978), and these theories all show dependencies for Li depletion on parameters of mass and age. The sample of halo stars may all be within 20% of each other's age and each other's mass, so that these dependencies would be masked. The mechanism of the depletion in Pop I stars is not well understood, and by analogy the situation in Pop II stars may be equally obscure. However, Michaud et al. (1984) and Michaud (1985) discuss diffusion in these stars and show that the near-constant Li/H value over the temperature range from 5500–6200 K is not consistent with diffusion, which has a dependency on stellar mass. Only if the mixing length to scale height ratio characterizing convection is allowed to change with time will the temperature at the bottom of the convection zone stay constant and the Li be uniformly depleted. (Note that depletion takes place at a similar interior temperature in the Pop I and Pop II stars, but the stellar mass at which the base of the convection zone reaches the critical temperature is lower in the Pop II stars.)

The Pop II Li/H value ($0.7\text{--}1.8 \times 10^{-10}$) probably represents a lower limit for ^7Li . The measured Li/H value in Pop I stars is a combination of Big Bang ^7Li plus GCR-produced ^7Li and ^6Li (and possibly additional contributions from other sources). If the Pop I abundance of 10^{-9} is

adopted and Li production by GCR spallation is $\sim 2 \times 10^{-10}$, then the upper limit to the Big Bang abundance of ${}^7\text{Li}$ would be 8×10^{-10} .

3.6 *Abundance Summary*

In order to make quantitative comparisons between theory and observation, it is necessary to infer from the data reasonably accurate estimates of (or limits to) the primordial abundances of the light elements. Although there have been impressive observational achievements, there is still progress to be made. For example, D has been observed only in the solar system and in the local (< 1 kpc) interstellar medium, and ${}^3\text{He}$ has been measured only in the solar system and in three galactic H II regions. A universal, primordial abundance for D and ${}^3\text{He}$ has to be deduced from such limited data. For lithium the observational situation is better; it has been observed in hundreds of Pop I stars of various ages (including the Sun), in roughly two dozen Pop II stars, in chondritic meteorites, and in the interstellar gas. There are problems here, too, since the observations of a uniform (predepletion) abundance of Li in the presolar nebula, in the present interstellar gas, and in Pop I stars of differing ages (10^6 – 10^9 yr) are hard to reconcile with the apparently uniform Pop II abundance. The status of the ${}^4\text{He}$ observations is much better. High-quality data (line widths determined to better than 10%) for galactic and, especially, extragalactic H II regions have been acquired in recent years. Qualitatively, a clear picture of a uniform, universal abundance, augmented by varying amounts of stellar-produced ${}^4\text{He}$, has emerged. The problem here is that exceedingly accurate (2–3%) values of the primordial abundances are required to test the predictions of the standard model. The necessity of correcting accurately for the unobserved neutral He and for the He produced in stars during the course of galactic evolution (in galaxies that may have evolved differently from each other) exacerbates the usual problems associated with the attainment of such precise abundances.

For deuterium, as discussed in Section 3.2, the step back from the observations to the primordial value is the most difficult. Observational guidance and chemical evolution models suggest depletions by factors of 2–10 from primordial to present D/H. Encompassing these limits around the range in the interstellar results gives

$$1.6 \times 10^{-5} < (\text{D}/\text{H})_{\text{p}} < 2 \times 10^{-4}.$$

To avoid conclusions whose origin is more in model assumptions than in observational data, we content ourselves with a conservative lower limit to the primordial abundance of deuterium:

$$(\text{D}/\text{H})_{\text{p}} > 1\text{--}2 \times 10^{-5}. \quad 20.$$

To derive upper limits for $(\text{D}/\text{H})_{\text{p}}$ and/or $({}^3\text{He}/\text{H})_{\text{p}}$ involves estimates

from uncertain models. Nonetheless, a high primordial D abundance would indicate that little of the interstellar gas could have avoided being processed through stars and that, furthermore, such efficient star formation would have overproduced ${}^3\text{He}$. YTSSO have shown how the solar system abundances of D and ${}^3\text{He}$ can be used to set upper limits on the sum of the primordial production of these elements. Accounting for the survival of ${}^3\text{He}$ and the conversion of D to ${}^3\text{He}$, but ignoring newly synthesized ${}^3\text{He}$, the solar system abundances suggest that

$$[(\text{D} + {}^3\text{He})/\text{H}]_p < 6\text{--}10 \times 10^{-5}. \quad 21.$$

The remarkably uniform maximum values for Li in Pop I stars of different ages, in the meteorites, and in the interstellar gas indicate that galactic evolution has had little effect (neither much production nor much destruction) on the primordial abundance. With the small correction for the well-established addition by galactic cosmic-ray spallation production, the primordial value from Pop I is within a factor of 2 of

$$({}^7\text{Li}/\text{H})_p = 8 \times 10^{-10} \text{ (Pop I)}. \quad 22a.$$

The recent discovery of a remarkably uniform Li abundance in 17 Pop II dwarfs suggests instead that the appropriate Li/H value is that for the Pop II stars:

$$({}^7\text{Li}/\text{H})_p = 0.7\text{--}1.8 \times 10^{-10} \text{ (Pop II)}. \quad 22b.$$

The above estimate has not allowed for any destruction of ${}^7\text{Li}$ prior to the formation of the Pop II stars observed by Spite et al. (1984). Inasmuch as D is more fragile than ${}^7\text{Li}$, it follows that

$$({}^7\text{Li}/\text{D})_p < {}^7\text{Li (Pop II)}/\text{D} < 1.5 \times 10^{-5}$$

(Austin & King 1977, Mathews & Viola 1979, YTSSO).

Until there is better understanding of the depletion processes in main-sequence stars, it is safest to include both possibilities for primordial ${}^7\text{Li}$, viz.

$$1 \times 10^{-10} < ({}^7\text{Li}/\text{H})_p < 8 \times 10^{-10}. \quad 23.$$

For ${}^4\text{He}$, all the high-quality data are consistent with $Y_p = 0.24 \pm 0.02$. It is likely that systematic effects—and not statistical uncertainties—dominate. For our best estimate of Y_p we follow Pagel (1984) and adopt the maximum likelihood solution from the study by Kunth & Sargent (1983), corrected for possible evolution and with account taken of the uncertainties associated with the ionization corrections and the chemical evolution correction (Steigman 1985):

$$Y_p = 0.239 \pm 0.015. \quad 24.$$

With the above estimates of the primordial abundances of the light elements, we may now make comparisons with the abundances predicted by the standard model and by variations on the model.

4. CONFRONTATION OF THEORY WITH DATA

Before we attempt a quantitative comparison of theory and observation, we note that there is excellent qualitative agreement between the predictions of the standard model and our inferred primordial abundances. This consistency is displayed in Figure 12, where we show the predictions for Y_p , D_p ,

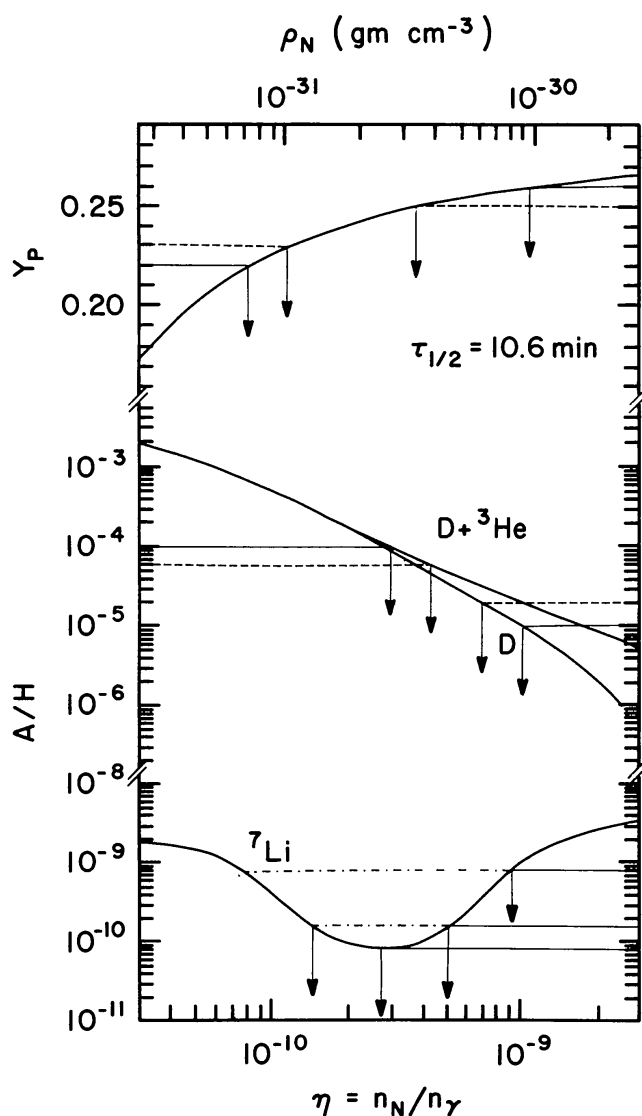


Figure 12 Comparison of the predicted and observed abundances. See text for discussion.

$(D + {}^3\text{He})_p$, and ${}^7\text{Li}_p$ (from Figure 2) in the standard model ($N_\nu = 3$, $\tau_n = 10.6$ min) and the adopted ranges of the primordial abundances. It is not unremarkable that the observed abundances of ${}^4\text{He}$, D , and ${}^7\text{Li}$ are predicted by the standard model for $\eta_{10} \approx 1$ – 10 .

4.1 The Standard Model

The *lower* limit to the deuterium abundance adopted in Equation 20 leads—in the standard model—to an *upper* limit to the nucleon abundance: $\eta_{10} < 7$ – 10 ; if we had chosen instead $(D/H)_p > 5 \times 10^{-6}$, then we would have had an upper limit of $\eta_{10} < 15$. A primordial ${}^7\text{Li}$ abundance from the Pop II stars of $< 1.8 \times 10^{-10}$ restricts the nucleon abundance to $1.5 < \eta_{10} < 5$. If some destruction of ${}^7\text{Li}$ before the halo stars formed is allowed for, so that $({}^7\text{Li}/D)_p < 1.5 \times 10^{-5}$, then $\eta_{10} < 7$. Taken together, primordial D and ${}^7\text{Li}$ (Pop II) restrict the nucleon abundance—in the standard model—to

$$\eta_{10} < 5\text{--}7 \text{ (D and Pop II } {}^7\text{Li}), \quad 25a.$$

or, if the lithium data are ignored,

$$\eta_{10} < 7\text{--}10 \text{ (D alone)}. \quad 25b.$$

On the other hand, a primordial ${}^7\text{Li}$ content from Pop I of 8×10^{-10} corresponds to $\eta_{10} < 9$ (and $\eta_{10} > 7$ when the lower bound for ${}^7\text{Li}$ of 5×10^{-10} is used with the GCR value of 2×10^{-10}), i.e.

$$\eta_{10} < 7\text{--}9 \text{ (Pop I } {}^7\text{Li}). \quad 25c.$$

The *upper* limit to the sum of the primordial abundances of deuterium and helium-3 imposes a *lower* limit to the nucleon-to-photon ratio:

$$\eta_{10} > 3\text{--}4 \text{ (D plus } {}^3\text{He}). \quad 26.$$

Comparing Equations 25 and 26, we see that there is a small range in nucleon abundance for which the predictions of the standard model are in agreement with the primordial abundances of D , ${}^3\text{He}$, and ${}^7\text{Li}$ inferred from the observational data.

For the parameters of the standard model and for η in the allowed range, the predicted abundance of primordial ${}^4\text{He}$ varies from $Y_p = 0.243$ to $Y_p = 0.255$ (see Table 1), in agreement with our estimate in Equation 24. If we take account of the current uncertainty in the neutron half-life, the standard model ($N_\nu = 3$) is, for $(D + {}^3\text{He})_p < 10^{-4}$, consistent with a ${}^4\text{He}$ primordial mass fraction as small as $Y_p = 0.240$ ($\tau_n = 10.4$ min) or $Y_p = 0.237$ ($\tau_n = 10.2$ min).

If the τ -neutrino is heavy ($m_{\nu\tau} \gg 25$ MeV), even smaller abundances of primordial ${}^4\text{He}$ are predicted; for $(D + {}^3\text{He})_p < 10^{-4}$, we have $Y_p(N_\nu \geq$

2) $> 0.229, 0.226, 0.223$ (for $\tau_\nu = 10.6, 10.4, 10.2$ min). Since the e^- and μ^- -neutrinos are *light*, it follows that $N_\nu \geq 2$; thus the “bottom line” is that the standard model would be incompatible with a primordial abundance $Y_p < 0.22$. The primordial abundance of ^4He —accurately determined—provides a “litmus test” of the standard hot Big Bang cosmology.

For $3-4 < \eta_{10} < 7-10$, the standard model synthesizes *all* light elements in abundances consistent with current data. This remarkable concordance lends strong support to the standard hot Big Bang model and provides evidence of its validity in describing the early evolution of the Universe. Given the quantitative success of the standard model, it is reasonable to require that any deviations from the underlying assumptions not spoil the good agreement between the theoretical predictions and the observational data. In this spirit, we investigate the constraints on possible alternatives to the standard model.

4.2 Limits to N'_ν and ξ

An increase in the early expansion rate ($\xi > 1$) due to additional species of light particles ($N'_\nu > 3$) or other effects (degeneracy, alternate theories of gravity, anisotropy, etc.) leads to an increase in the primordial abundances of D, ^3He , and ^4He . If we require that $Y_p < 0.254$ (Equation 24) and that $[(\text{D} + ^3\text{He})/\text{H}]_p < 10^{-4}$ (Equation 21), then a constraint on N'_ν follows from Equation 14:

$$N'_\nu < 3.8 - (\tau_n - 10.6). \quad 27.$$

With $\tau_n > 10.4$ min, we find that $N'_\nu < 4$, so that at most only one extra species of light, two-component particle is allowed (YSSR, Steigman et al. 1979, OSSTY, YTSSO).

This limit to N'_ν is equivalent to an upper bound to the speedup factor (see Equation 13):

$$\xi - 1 < 0.062 - 0.076(\tau_n - 10.6). \quad 28.$$

Any permissible speedup in the early expansion rate is constrained to be small; for $\tau_n > 10.4$ min, we have $\xi - 1 < 0.08$. This constraint on ξ is responsible for the severe limitations to variations on the theme of the standard model discussed in Section 2.4.

5. COSMOLOGICAL CONSTRAINTS

The predictions of the standard model ($N_\nu = 3$, $\tau_n = 10.6 \pm 0.2$ min) are in agreement with the estimates of the primordial abundances derived from the observational data, provided that the nucleon abundance (the nucleon-to-photon ratio today) is either in the range $3-4 < \eta_{10} < 7-10$ (without ^7Li)

or in the range $3-4 < \eta_{10} < 5-9$ (with ${}^7\text{Li}$). The present number density of relic (i.e. microwave, blackbody) photons is

$$n_{\gamma 0} = 399(T_{\gamma 0}/2.7)^3 \equiv 399\theta^3 \text{ cm}^{-3}. \quad 29.$$

In Equation 29, $T_{\gamma 0}$ is the present temperature of the microwave background radiation ($2.7 < T_{\gamma 0} < 3.0$ K), and θ is $T_{\gamma 0}$ in units of 2.7 K. The present nucleon mass density is

$$\rho_{N0} = M_N \eta n_{\gamma 0} = 6.63 \times 10^{-32} \theta^3 \eta_{10} \text{ g cm}^{-3}. \quad 30.$$

The present value of the “critical” (Einstein–de Sitter) density (see Section 2) is

$$\rho_{c0} = 3H_0^2/8\pi G = 1.88 \times 10^{-29} h_0^2 \text{ g cm}^{-3}, \quad 31.$$

where the present value of the Hubble parameter is $H_0 = 100 h_0 \text{ km s}^{-1} \text{ Mpc}^{-1}$; it is likely that $1/2 < h_0 < 1$ (Sandage & Tammann 1982, Buta & de Vaucouleurs 1983, Aaronson & Mould 1983), but values as small as $h_0 \simeq 0.4$ cannot be excluded (Branch et al. 1983). The fraction of the critical density in nucleons is

$$\Omega_N = \rho_N/\rho_c = 0.00353 h_0^{-2} \theta^3 \eta_{10}. \quad 32.$$

Accounting for the uncertainties in H_0 ($1/2 < h_0 < 1$) and $T_{\gamma 0}$ ($1 < \theta < 1.11$), we find that

$$0.00353 \eta_{10} < \Omega_N < 0.0194 \eta_{10}. \quad 33.$$

If H_0 as small as $40 \text{ km s}^{-1} \text{ Mpc}^{-1}$ is admitted, the upper limit on Ω_N increases to $\Omega_N < 0.030 \eta_{10}$.

5.1 Lower Bound to the Nucleon Density

The requirement that deuterium not be overproduced in Big Bang nucleosynthesis has led us to place a *lower* bound on the nucleon abundance of $\eta_{10} > 3-4$. The present nucleon mass density, therefore, is bounded from below by

$$\rho_{N0} > 2-3 \times 10^{-31} \text{ g cm}^{-3}; \quad \Omega_N > 0.011-0.014. \quad 34.$$

The conventional approach to estimating the universal mass density is via dynamics—through an application of Newton’s laws of motion (see, for example, Faber & Gallagher 1979). Current data suggest that the material associated with the inner, *luminous* parts of galaxies contributes $\Omega_{\text{Gal}} \approx 0.01-0.02$ (see YTSSO). It is far from trivial that our independent estimate of the (nucleon) mass density—based on primordial nucleosynthesis—is comparable to the mass density associated with galaxies—as determined by Newtonian dynamics.

5.2 *Upper Bound to the Nucleon Density*

The requirement that Big Bang nucleosynthesis produce deuterium in (at least) its presently observed abundance led us to place an *upper* bound on the nucleon abundance of $\eta_{10} < 7\text{--}10$. The present mass density in nucleons, therefore, is bounded from above by

$$\rho_{\text{N}0} < 6\text{--}9 \times 10^{-31} \text{ g cm}^{-3}; \quad \Omega_{\text{N}} < 0.14\text{--}0.19. \quad 35.$$

If $h_0 \approx 0.4$ is admitted, the upper limit on Ω_{N} increases to $\Omega_{\text{N}} < 0.21\text{--}0.30$.

If the ${}^7\text{Li}$ abundance derived from the Pop II stars provides a good estimate of the primordial abundance of ${}^7\text{Li}$, then the upper bound on the nucleon-to-photon ratio is reduced ($\eta_{10} < 5\text{--}7$). In this case, we have $\Omega_{\text{N}} < 0.10\text{--}0.14$ (for $h_0 > 1/2$) or $\Omega_{\text{N}} < 0.15\text{--}0.21$ ($h_0 > 0.4$).

It is well established that *most* of the mass associated with galaxies is nonluminous, i.e. “dark” (see Faber & Gallagher 1979). The mass density inferred from the study of the dynamics of galaxies on the largest scales (groups, clusters, superclusters, etc.) is $\Omega_{\text{dyn}} \approx 0.2 \pm 0.1$ (for an excellent summary, see Peebles 1984). Nucleons, then, are capable of accounting for most—perhaps all—the mass *yet observed* in the Universe. Only if it is established that $\Omega_0 > 0.2\text{--}0.3$ will it be necessary to invoke massive neutrinos or other exotic relics from the Big Bang.

5.3 *Can Nucleons “Close” the Universe?*

The “naturalness” of the Einstein–de Sitter model ($k = \Lambda = 0$, $\Omega_0 = 1$) suggests that the universal mass density be equal to the critical value. Inflationary universe scenarios (Guth 1981, Linde 1982, Albrecht & Steinhardt 1982) ensure that the curvature term (see Equation 1) is negligible today, so that $\Omega_0 \approx 1$ if $\Lambda \ll 3H_0^2$. Is an Einstein–de Sitter universe compatible with a nucleon-dominated universe ($\Omega_{\text{N}} = \Omega_0 = 1$)? No! Not if the successes of Big Bang nucleosynthesis are to be preserved. We have already seen that even for H_0 as small as $40 \text{ km s}^{-1} \text{ Mpc}^{-1}$ and η_{10} as large as 10 (and $T_{\gamma 0} = 3 \text{ K}$), we have $\Omega_{\text{N}} < 0.3$. More typically, the nucleon density fails by a factor larger than 7–10 to “close” the Universe.

Indeed, if $h_0 > 1/2$, then $\eta_{10} > 52$ is required if $\Omega_{\text{N}} = 1$. For such a large nucleon abundance, the primordial abundance of deuterium would fail to account for that observed by some two orders of magnitude, while the primordial abundance of lithium would exceed that observed by one (Pop I) or two (Pop II) orders of magnitude; in this case, $Y_p > 0.27$ is also predicted (Steigman 1985). Even if H_0 is as small as $40 \text{ km s}^{-1} \text{ Mpc}^{-1}$, $\eta_{10} > 33$ is required and similar discrepancies are predicted (see Figure 2).

6. CONCLUSIONS AND FURTHER RESEARCH

The abundances predicted from nucleosynthesis by the standard model of the hot Big Bang are given in Section 2.2 and Table 1. The observations of the light isotopes ^2H , ^3He , ^4He , and ^7Li are presented in Section 3 and summarized in Section 3.6. The predictions and observations are compared in Section 4, and the consequences for cosmology are discussed in Section 5. The agreement between the standard model predictions and the observationally inferred primordial abundances is good. However, there are some areas where the predictions could be improved and where the observations could further test the theory.

The cross sections for the nuclear reactions involving Li production and destruction are the least well known. More accurate values are needed for $^7\text{Li}(p, \alpha)^4\text{He}$, $^3\text{He}(\alpha, \gamma)^7\text{Be}$, and $^7\text{Be}(n, p)^7\text{Li}$. A better estimate of the neutron half-life would reduce the uncertainty in the Y_p predictions.

For D, the major uncertainty is the amount of processing that has taken place, i.e. how to infer the primordial value from the local present-day D measurements. Here more ultraviolet absorption studies of D in the Galaxy and in front of extragalactic objects are needed (see, for example, York et al. 1984). Additional work on the probable H I “puffs” from B stars could determine the magnitude and constancy of the possible contamination of the interstellar D lines by stellar H.

Helium-3 is primarily observed locally, and its abundance depends on knowledge of the solar ^4He content, which is known only to $\pm 20\%$. More observations like those of Rood et al. (1984) of $^3\text{He}^+$ in galactic H II regions would be useful.

The best source of ^4He abundances appears to be extragalactic H II regions. Knowledge of the evolution of the ^4He abundance with time can be circumvented by searching for and carefully observing very low metal extragalactic H II regions. New insights on the corrections for neutral He may be found in detailed studies of local H II regions, possibly with variable slit dimensions.

In the case of ^7Li the major issue is the resolution of the Pop I maximum vs. the Pop II mean for the primordial ^7Li content. Observations of ^7Li in additional halo dwarfs is one obvious approach. A search for spatial variations in Li in galactic disk stars of various ages might reveal whether the ^7Li content of the disk has increased with time (as suggested if the Pop II ^7Li is primordial) or is unchanged (or slightly decreased) with time (as suggested by the observed Li depletions in Pop I stars).

The primary observational techniques used to determine the abundances of these four light isotopes are very different (e.g. interstellar UV absorption

studies, optical recombination emission spectra, photospheric absorption lines), yet the consistency of the cosmological results is remarkable. Further clarifications and refinements will be forthcoming with additional observations and theoretical understanding of stellar and galactic evolution.

ACKNOWLEDGMENTS

We are indebted to a number of colleagues for stimulating discussions, letters, and preprints of their work. In particular, we thank Drs. J. Audouze, J. Barrow, K. Davidson, D. Duncan, D. Kunth, R. Matzner, M. Peimbert, and D. York. We have also profited from the advice and wisdom of Drs. J. Gallagher, G. Herbig, L. Hobbs, B. Pagel, H. Reeves, R. Rood, D. Schramm, P. Shaver, J. Truran, and M. Turner. We are especially grateful to Jean Audouze, Claudine Laurent, Francois Spite, and Brent Tully for their comments on various parts of the manuscript. AMB acknowledges with appreciation the hospitality of the Berkeley Astronomy Department, where she spent much of her time during the preparation of this review article. This work is supported at Bartol by Department of Energy grant DE-AC02-78ER-05007, and at Hawaii by National Science Foundation grant AST 82-16192. It is a pleasure to thank Louise Good of the Institute for Astronomy for her skill and efficiency at typing and revising the manuscript, often via long distance.

Literature Cited

- Aaronson, M., Mould, J. 1983. *Ap. J.* 265:1
 Albrecht, A., Steinhardt, P. J. 1982. *Phys. Rev. Lett.* 48:1220
 Alloin, D., Cruz-Gonzalez, G., Peimbert, M. 1976. *Ap. J.* 205:74
 Alschuler, W. R. 1975. *Ap. J.* 195:649
 Anantharamaiah, K. R., Radhakrishnan, V. 1979. *Astron. Astrophys.* 79:L9
 Anders, E., Ebihara, M. 1982. *Geochim. Cosmochim. Acta* 46:2363
 Anderson, R. C., Henry, R. C., Moos, H. W., Linsky, J. L. 1978. *Ap. J.* 226:883
 Anderson, R. C., Weiler, E. J. 1978. *Ap. J.* 224:143
 Arnould, M., Nørgaard, H. 1975. *Astron. Astrophys.* 42:55
 Audouze, J. 1984. Paper presented at ESO-CERN Symp. Large Scale Struct. Universe, Cosmology, Fundam. Phys., 1st
 Audouze, J., Boulade, O., Malinie, G., Poilane, Y. 1983. *Astron. Astrophys.* 127:164
 Audouze, J., Tinsley, B. M. 1974. *Ap. J.* 192:487
 Audouze, J., Tinsley, B. M. 1976. *Ann. Rev. Astron. Astrophys.* 14:43
 Audouze, J., Truran, J. W. 1973. *Ap. J.* 182:839
 Auer, L., Mihalas, D. 1973. *Ap. J. Suppl.* 25:433
 Austin, S. M., King, C. H. 1977. *Nature* 269:782
 Bahcall, J. N., Huebner, W. F., Lubow, S. H., Parker, P. D., Ulrich, R. K. 1982. *Rev. Mod. Phys.* 54:767
 Baliunas, S. L., Dupree, A. K. 1979. *Ap. J.* 227:870
 Barker, T. 1978. *Ap. J.* 220:193
 Barrow, J. D. 1976. *MNRAS* 175:359
 Barrow, J. D. 1977. *MNRAS* 178:625
 Barrow, J. D. 1978. *MNRAS* 184:677
 Barrow, J. D., Morgan, J. 1983. *MNRAS* 203:393
 Beaudet, G., Goret, P. 1976. *Astron. Astrophys.* 49:415
 Beaudet, G., Reeves, H. 1983. See Shaver et al. 1983a, p. 53
 Beaudet, G., Yahil, A. 1977. *Ap. J.* 218:253

- Bekenstein, J. D. 1977. *Phys. Rev. D* 15: 1458
- Bekenstein, J. D., Meisels, A. 1980. *Ap. J.* 237: 342
- Black, D. C. 1971. *Nature Phys. Sci.* 234: 148
- Black, D. C. 1972. *Geochim. Cosmochim. Acta* 36: 347
- Black, D. C. 1973. *Icarus* 19: 154
- Bodenheimer, P. 1965. *Ap. J.* 142: 451
- Bodenheimer, P. 1966. *Ap. J.* 144: 103
- Boesgaard, A. M. 1970. *Ap. J.* 161: 1003
- Boesgaard, A. M. 1971. *Ap. J.* 167: 511
- Boesgaard, A. M. 1976. *Publ. Astron. Soc. Pac.* 88: 353
- Boesgaard, A. M., Heacox, W. D., Conti, P. S. 1977. *Ap. J.* 214: 124
- Boesgaard, A. M., Tripicco, M. J. 1985. Submitted for publication
- Bondarenko, L. N., Kurguzov, V. V., Prokofiev, Yu. A., Rogov, E. V., Spivak, P. E. 1978. *JETP Lett.* 28: 303
- Bopp, P., Dubbers, D., Klemm, E., Last, J., Schultze, H. 1984. *J. Phys. (Paris)* 45: C3
- Branch, D., Lacy, C. H., McCall, M. L., Sutherland, P. G., Uomoto, A., et al. 1983. *Ap. J.* 270: 123
- Brans, C., Dicke, R. H. 1961. *Phys. Rev.* 124: 925
- Bruston, P., Audouze, J., Vidal-Madjar, A., Laurent, C. 1981. *Ap. J.* 243: 161
- Buta, R., de Vaucouleurs, G. 1983. *Ap. J.* 266: 1
- Buzzoni, A., Fusi Pecci, F., Buohanno, R., Corsi, C. E. 1983. See Shaver et al. 1983a, p. 231
- Byrne, J. 1984. *Nature* 310: 212
- Byrne, J., Morse, J., Smith, K. F., Shaikh, F., Green, K., et al. 1980. *Phys. Lett. B* 92: 274
- Cambier, J.-L., Primack, J. R., Sher, M. 1982. *Nucl. Phys. B* 209: 372
- Cameron, A. G. W. 1955. *Ap. J.* 121: 144
- Cameron, A. G. W. 1982. In *Essays in Nuclear Astrophysics*, ed. C. A. Barnes, D. D. Clayton, D. N. Schramm, p. 23. Cambridge: Cambridge Univ. Press
- Cameron, A. G. W., Fowler, W. A. 1971. *Ap. J.* 164: 111
- Canal, R. 1974. *Ap. J.* 189: 531
- Canal, R., Isern, J., Sanahuja, B. 1975. *Ap. J.* 200: 646
- Canal, R., Isern, J., Sanahuja, B. 1980. *Ap. J.* 235: 504
- Cannon, R. D. 1983. See Shaver et al. 1983a, p. 223
- Caputo, F., Castellani, V. 1983. See Shaver et al. 1983a, p. 213
- Caputo, F., Cayrel de Strobel, G. 1981. In *Astrophysical Parameters for Globular Clusters*, IAU Colloq. No. 68, ed. A. G. Davis Philip, D. S. Hayes, p. 415. Schnectady, NY: L. Davis
- Carney, R. W. 1983. See Shaver et al. 1983a, p. 179
- Carswell, R. F. 1969. *MNRAS* 144: 279
- Cayrel, R., Cayrel de Strobel, G., Campbell, B., Dappen, W. 1984. *Ap. J.* 283: 205
- Cesarsky, D. A., Moffet, A. T., Pasachoff, J. M. 1973. *Ap. J. Lett.* 186: L1
- Christensen, C. J., Nielsen, A., Bahnsen, A., Brown, W. K., Rustad, B. M. 1972. *Phys. Rev. D* 5: 1628
- Christensen-Dalsgaard, J., Gough, D. O. 1980. *Nature* 288: 544
- Clayton, D. D. 1985. *Ap. J.* 290: 428
- Cole, P. W., Demarque, P., Green, E. M. 1983. See Shaver et al. 1983a, p. 235
- Conrath, B., Gautier, D., Hornstein, J. 1982. Presented at Saturn Conf., Tucson, Ariz.
- D'Antona, F., Mazzitelli, M. 1984. *Astron. Astrophys.* 138: 431
- David, Y., Reeves, H. 1980. In *Physical Cosmology*, ed. R. Balian, J. Audouze, D. N. Schramm, p. 433. Amsterdam: North-Holland
- Davidson, K., Kinman, T. D. 1985. *Ap. J.* In press
- Dean, C. A., Lee, P., O'Brien, A. 1977. *Publ. Astron. Soc. Pac.* 89: 222
- Dearborn, D. S. P., Blake, J. B., Hainebach, K. L., Schramm, D. N. 1978. *Ap. J.* 223: 552
- Delbourgo-Salvador, P., Gry, C., Malinie, G., Audouze, J. 1985. Submitted for publication
- Dicke, R. H. 1968. *Ap. J.* 152: 1
- Dicus, D. A., Kolb, E. W., Gleeson, A. M., Sudarshan, E. C. G., Teplitz, V. L., et al. 1982. *Phys. Rev. D* 26: 2694
- Dicus, D. A., Teplitz, V. L. 1980. *Phys. Rev. Lett.* 44: 218
- Duncan, D. K. 1981. *Ap. J.* 248: 651
- Duncan, D. K., Jones, B. F. 1983. *Ap. J.* 271: 663
- Dupree, A. K., Baliunas, S. L., Shipman, H. L. 1977. *Ap. J.* 218: 361
- Eberhardt, P. 1978. *Proc. Lunar Planet. Sci. Conf., 9th*, p. 1027
- Encrenaz, T., Combes, M. 1982. *Icarus* 52: 54
- Epstein, R. I., Petrosian, V. 1975. *Ap. J.* 197: 281
- Eroozlimskii, B. G., Frank, A. I., Mostovoi, Yu. A., Arzumanov, S. S., Voitzik, L. R. 1979. *Sov. J. Nucl. Phys.* 30: 356
- Faber, S. M., Gallagher, J. S. 1979. *Ann. Rev. Astron. Astrophys.* 17: 135
- Ferlet, R., Dennefeld, M. 1984. *Astron. Astrophys.* 138: 303
- Ferlet, R., Dennefeld, M., Spite, M. 1983. *Astron. Astrophys.* 124: 172
- Ferlet, R., Gry, C., Vidal-Madjar, A. 1985. In *Local Interstellar Medium*, IAU Colloq. No. 81. In press
- Ferlet, R., Vidal-Madjar, A., Laurent, C., York, D. G. 1980. *Ap. J.* 242: 576
- Fowler, W. A., Caughlan, G. R., Zimmerman, B. A. 1975. *Ann. Rev. Astron. Astrophys.* 13: 69

- French, H. B. 1980. *Ap. J.* 240:41
 French, H. B. 1981. *Ap. J.* 246:34
 French, H. B., Miller, J. S. 1981. *Ap. J.* 248:468
 Frick, U., Moniot, R. K. 1977. *Proc. Lunar Sci. Conf., 8th*, p. 229
 Fry, J. N., Hogan, C. J. 1982. *Phys. Rev. Lett.* 49:1873
 Gaupp, A., Kuske, P., Andra, H. J. 1982. *Phys. Rev. A* 26:3351
 Gautier, D. 1983. See Shaver et al. 1983a, p. 139
 Gautier, D., Conrath, B., Flasar, M., Hanel, R., Kunde, V., et al. 1981. *J. Geophys. Res.* 86:8713
 Geiss, J. 1982. *Space Sci. Rev.* 33:201
 Geiss, J., Eberhardt, P., Bühler, F., Meister, J., Signer, P. 1970. *J. Geophys. Res.* 75:5972
 Geiss, J., Reeves, H. 1972. *Astron. Astrophys.* 18:126
 Geiss, J., Reeves, H. 1981. *Astron. Astrophys.* 93:189
 Giampapa, M. S. 1984. *Ap. J.* 277:235
 Gisler, G. R., Harrison, E. R., Rees, M. J. 1974. *MNRAS* 166:663
 Gough, D. O. 1983. See Shaver et al. 1983a, p. 117
 Grec, G., Fossat, E., Pomerantz, M. A. 1980. *Nature* 288:541
 Grec, G., Fossat, E., Pomerantz, M. A. 1983. *Sol. Phys.* 82:55
 Greenstein, G. 1968. *Astrophys. Space Sci.* 2:155
 Gry, C., Lamers, H. J. G. L. M., Vidal-Madjar, A. 1984. *Astron. Astrophys.* 137:29
 Gry, C., Laurent, C., Vidal-Madjar, A. 1983a. *Astron. Astrophys.* 124:99
 Gry, C., Malinie, G., Audouze, J., Vidal-Madjar, A. 1983b. In *Formation and Evolution of Galaxies and Large Structures in the Universe*, ed. J. Audouze, J. Tran Than Van, p. 279. Dordrecht: Reidel
 Guth, A. H. 1981. *Phys. Rev. D* 23:347
 Harris, M. J., Fowler, W. A., Caughlan, G. R., Zimmerman, B. A. 1983. *Ann. Rev. Astron. Astrophys.* 21:165
 Hawking, S. W., Tayler, R. J. 1966. *Nature* 209:1278
 Hawley, S. A. 1978. *Ap. J.* 224:417
 Heasley, J. N., Milkey, R. 1978. *Ap. J.* 221:677
 Heasley, J. N., Wolff, S. C., Timothy, J. G. 1982. *Ap. J.* 262:663
 Herbig, G. H., Wolff, R. J. 1966. *Ann. Astrophys.* 29:593
 Hobbs, L. M. 1969. *Ap. J.* 157:135
 Hobbs, L. M. 1984. *Ap. J.* 286:252
 Hubbard, W. B., MacFarlane, J. J. 1980. *Icarus* 44:676
 Iben, I. Jr. 1965. *Ap. J.* 142:1447
 Iben, I. Jr. 1967. *Ap. J.* 147:624, 650
 Iben, I. Jr. 1968. *Nature* 220:143
 Jeffrey, P. M., Anders, E. 1970. *Geochim. Cosmochim. Acta* 34:1175
 Johansson, A. E. I., Peressutti, G., Shagerstam, B.-S. K. 1982. *Phys. Lett. B* 117:171
 Keenan, F. P., Dufton, P. L., McKeith, C. D. 1982. *MNRAS* 200:673
 Kinman, T. D., Davidson, K. 1981. *Ap. J.* 243:127
 Kolb, E. W., Sherrer, R. J. 1982. *Phys. Rev. D* 25:1481
 Krohn, V. E., Ringo, G. R. 1975. *Phys. Lett. B* 55:175
 Kunde, V., Hanel, R., Maguire, W., Gautier, D., Baluteau, J. P., et al. 1982. *Ap. J.* 263:443
 Kunth, D. 1983. See Shaver et al. 1983a, p. 305
 Kunth, D., Sargent, W. L. W. 1983. *Ap. J.* 273:81
 Lambert, D. L., Dominy, J. F., Sivertsen, S. 1980. *Ap. J.* 235:114
 Lambert, D. L., Sawyer, S. R. 1984. *Ap. J.* 283:192
 Lambert, D. L., Luck, R. E. 1978. *MNRAS* 183:79
 Laurent, C. 1983. See Shaver et al. 1983a, p. 335
 Laurent, C., Vidal-Madjar, A., York, D. G. 1979. *Ap. J.* 229:923
 Lequeux, J., Peimbert, M., Rayo, J. F., Serrano, A., Torres-Peimbert, S. 1979. *Astron. Astrophys.* 80:155
 Linde, A. D. 1982. *Phys. Lett. B* 108:389
 Maeder, A. 1983. See Shaver et al. 1983a, p. 89
 Mathews, G. J., Viola, V. E. 1979. *Ap. J.* 228:375
 Matzner, R. 1984. In *Numerical Astrophysics*, ed. J. Centrella, J. Le Blanc, R. Bowers. Boston: Jones & Bartlett. In press
 Maurice, E., Spite, F., Spite, M. 1984. *Astron. Astrophys.* 132:278
 Mazzitelli, I., Moretti, M. 1980. *Ap. J.* 235:955
 McClintock, W., Henry, R. C., Linsky, J. L., Moos, H. W. 1978. *Ap. J.* 225:465
 McKee, C. F., Ostriker, J. P. 1977. *Ap. J.* 218:148
 Meisels, A. 1982. *Ap. J.* 252:403
 Meneguzzi, M., Audouze, J., Reeves, H. 1971. *Astron. Astrophys.* 15:337
 Meneguzzi, M., Reeves, H. 1975. *Astron. Astrophys.* 40:99
 Merchant, A. M. 1967. *Ap. J.* 147:587
 Michaud, G. 1985. *Proc. Homestake Conf. Sol. Neutrinos and Neutrino Astron.*, ed. K. Lande. New York: Am. Inst. Phys. In press
 Michaud, G., Fontaine, G., Beaudet, G. 1984. *Ap. J.* 282:206
 Mihalas, D., Barnard, A. J., Cooper, J., Smith, E. G. 1974. *Ap. J.* 190:315
 Mihalas, D., Barnard, A. J., Cooper, J., Smith, E. G. 1975. *Ap. J.* 197:139

- Molaro, P., Beckman, J. E. 1984. *Astron. Astrophys.* 139:394
- Muller, E. A., Peytremann, E., de la Reza, R. 1975. *Sol. Phys.* 41:53
- Nichiporuk, W., Moore, C. B. 1974. *Geochim. Cosmochim. Acta* 38:1691
- Nissen, P. E. 1974. *Astron. Astrophys.* 36:57
- Nissen, P. E. 1976. *Astron. Astrophys.* 50:343
- Nissen, P. E. 1983. See Shaver et al. 1983a, p. 163
- Nørgaard, H., Fricke, K. J. 1976. *Astron. Astrophys.* 49:337
- Norris, J. 1971. *Ap. J. Suppl.* 23:193
- Novikov, I. D. 1971. *Sov. Astron. AJ* 14:960
- Olive, K. A., Schramm, D. N., Steigman, G. 1981a. *Nucl. Phys. B* 180:497
- Olive, K. A., Schramm, D. N., Steigman, G., Turner, M. S., Yang, J. 1981b. *Ap. J.* 246:557 (OSSTY)
- Olson, D. 1978. *Ap. J.* 219:777
- Osterbrock, D. E. 1974. *Astrophysics of Gaseous Nebulae*. San Francisco: Freeman. 251 pp.
- Pagel, B. E. J. 1982. *Philos. Trans. R. Soc. London Ser. A* 307:19
- Pagel, B. E. J. 1984. *Proc. Inner Space/Outer Space Workshop*. Batavia, Ill: Fermilab. In press
- Pasachoff, J. M., Cesarsky, D. A. 1974. *Ap. J.* 193:65
- Peebles, P. J. E. 1984. *Ap. J.* 284:439
- Peimbert, M. 1971. *Bol. Obs. Tonantzintla Tacubaya* 6:29
- Peimbert, M. 1983. See Shaver et al. 1983a, p. 267
- Peimbert, M., Costero, R. 1969. *Bol. Obs. Tonantzintla Tacubaya* 5:3
- Peimbert, M., Serrano, A. 1980. *Rev. Mex. Astron. Astrofis.* 5:9
- Peimbert, M., Torres-Peimbert, S. 1974. *Ap. J.* 193:327
- Peimbert, M., Torres-Peimbert, S. 1977. *MNRAS* 179:217
- Peimbert, M., Torres-Peimbert, S., Rayo, J. F. 1978. *Ap. J.* 220:516
- Peimbert, M., Wallerstein, G. 1965. *Ap. J.* 142:1024
- Peimbert, M., Wallerstein, G., Pilachowski, C. A. 1981. *Astron. Astrophys.* 104:72
- Penzias, A. A. 1979. *Ap. J.* 228:430
- Perrin, M.-N. 1983. See Shaver et al. 1983a, p. 209
- Pilachowski, C. A., Mould, J. R., Seigel, M. J. 1984. *Ap. J. Lett.* 282:L17
- Pradham, A. K. 1978. *MNRAS* 184:18P
- Predmore, C. R., Goldwire, H. C., Walters, G. K. 1971. *Ap. J. Lett.* 168:L125
- Rayo, J. F., Peimbert, M., Torres-Peimbert, S. 1982. *Ap. J.* 255:1
- Reeves, H. 1974. *Ann. Rev. Astron. Astrophys.* 12:437
- Renzini, A. 1983. See Shaver et al. 1983a, p. 109
- Renzini, A., Voli, M. 1981. *Astron. Astrophys.* 94:175
- Robbins, R. R. 1968. *Ap. J.* 151:511
- Rogerson, J. B., York, D. G. 1973. *Ap. J. Lett.* 186:L97
- Rood, R. T. 1972. *Ap. J.* 177:681
- Rood, R. T., Bania, T. M., Wilson, T. L. 1984. *Ap. J.* 280:629
- Rood, R. T., Steigman, G., Tinsley, B. M. 1976. *Ap. J. Lett.* 207:L57
- Rood, R. T., Wilson, T. L., Steigman, G. 1979. *Ap. J. Lett.* 227:L97
- Rosa, M. 1983. See Shaver et al. 1983a, p. 317
- Rothman, T., Matzner, R. 1984. *Phys. Rev. D* 30:1649
- Sackmann, I. J., Smith, R. L., Despain, K. H. 1974. *Ap. J.* 187:555
- Sandage, A., Tammann, G. A. 1982. *Ap. J.* 256:339
- Sargent, W. L. W., Searle, L. 1970. *Ap. J. Lett.* 162:L115
- Sarma, N. V. G., Mohanty, D. K. 1978. *MNRAS* 184:181
- Scalo, J. M., Despain, K. H., Ulrich, R. K. 1975. *Ap. J.* 196:805
- Scalo, J. M., Ulrich, R. K. 1973. *Ap. J.* 183:151
- Schatzman, E., Maeder, A. 1981. *Astron. Astrophys.* 96:1
- Schramm, D. N., Steigman, G. 1984. *Phys. Lett. B* 141:337
- Schramm, D. N., Wagoner, R. V. 1977. *Ann. Rev. Nucl. Part. Sci.* 27:37
- Searle, L., Sargent, W. L. W. 1972. *Ap. J.* 173:25
- Shaver, P. A. 1983. See Shaver et al. 1983a, p. 299
- Shaver, P. A., Kunth, D., Kjær, K., eds. 1983a. *ESO Workshop on Primordial Helium*. Garching: ESO. 422 pp.
- Shaver, P. A., McGee, M. X., Newton, L. M., Danks, A. C., Pottasch, S. R. 1983b. *MNRAS* 204:53
- Shvartsman, V. F. 1969. *JETP Lett.* 9:184
- Snell, R. L., Vanden Bout, P. A. 1981. *Ap. J.* 250:160
- Snell, R. L., Wooten, A. 1979. *Ap. J.* 228:748
- Spite, F., Spite, M. 1982a. *Astron. Astrophys.* 115:357
- Spite, M., Spite, F. 1982b. *Nature* 297:483
- Spite, M., Maillard, J. P., Spite, F. 1984. *Astron. Astrophys.* 141:56
- Starrfield, S., Truran, J. W., Sparks, W. M., Arnould, M. 1978. *Ap. J.* 222:600
- Stasinska, G. 1983. See Shaver et al. 1983a, p. 255
- Steigman, G. 1976. *Nature* 261:479
- Steigman, G. 1979. *Ann. Rev. Nucl. Part. Sci.* 29:313
- Steigman, G. 1985. In preparation
- Steigman, G., Olive, K. A., Schramm, D. N. 1979. *Phys. Rev. Lett.* 43:239

- Steigman, G., Schramm, D. N., Gunn, J. E. 1977. *Phys. Lett. B* 66:202
- Stratowa, C., Dobrozemsky, R., Weinziert, P. 1978. *Phys. Rev. D* 18:3970
- Straus, J. M., Blake, J. B., Schramm, D. N. 1976. *Ap. J.* 204:481
- Strömgren, B., Olsen, E. H., Gustafsson, B. 1982. *Publ. Astron. Soc. Pac.* 94:5
- Talbot, R. J., Arnett, W. E. 1973. *Ap. J.* 186:51, 69
- Talent, D. L., Dufour, R. J. 1979. *Ap. J.* 233:888
- Thorne, K. S. 1967. *Ap. J.* 148:51
- Tinsley, B. M. 1977. *Ap. J.* 216:548
- Torres-Peimbert, S., Wallerstein, G. 1966. *Ap. J.* 146:724
- Torres-Peimbert, S., Peimbert, M. 1977. *Rev. Mex. Astron. Astrofis.* 2:181
- Trafton, L., Ramsay, P. A. 1980. *Icarus* 41:423
- Traub, W. A., Carleton, N. P. 1973. *Ap. J. Lett.* 184:L11
- Truran, J. W. 1984. *Ann. Rev. Nucl. Part. Sci.* 34:53
- Truran, J. W., Brunish, W. 1985. In preparation
- Tully, R. B., Boesgaard, A. M., Dyck, H. M., Schempp, W. V. 1981. *Ap. J.* 246:38
- VandenBerg, D. A. 1983. *Ap. J. Suppl.* 51:29
- Vanden Bout, P. A., Grupsmith, G. 1974. *Ap. J. Lett.* 187:L9
- Vanden Bout, P. A., Snell, R. L., Vogt, S. S., Tull, R. G. 1978. *Ap. J.* 221:598
- Vauclair, S., Vauclair, G., Schatzman, E., Michaud, G. 1978. *Ap. J.* 223:567
- Vidal-Madjar, A. 1983. In *Diffuse Matter in Galaxies*, ed. J. Audouze, p. 57. Dordrecht: Reidel
- Vidal-Madjar, A., Ferlet, R., Laurent, C., York, D. G. 1982. *Ap. J.* 260:128
- Vidal-Madjar, A., Laurent, C., Bonnet, R. M., York, D. G. 1977. *Ap. J.* 211:91
- Vidal-Madjar, A., Laurent, C., Gry, C., Bruston, P., Ferlet, R., York, D. G. 1983. *Astron. Astrophys.* 120:58
- Vigroux, L., Arnould, M. 1979. *Int. Colloq., Liège, 22nd*, p. 47
- Wagoner, R. V. 1973. *Ap. J.* 179:343
- Wagoner, R. V. 1974. In *Confrontation of Cosmological Theories with Observational Data*, ed. M. S. Longair, p. 195. Dordrecht: Reidel
- Wagoner, R. V., Fowler, W. A., Hoyle, F. 1967. *Ap. J.* 148:3
- Wallerstein, G., Sneden, D. 1982. *Ap. J.* 255:577
- Weinberg, S. 1977. *The First Three Minutes*. New York: Basic Books. 188 pp.
- Wiese, W. L., Smith, M. W., Glennon, B. M. 1966. *Atomic Transition Probabilities, NSRDS-NBS4*, Vol. 1. Washington, DC: US Gov. Print. Off.
- Will, C. M. 1984. *Proc. Inner Space/Outer Space Workshop*. Batavia, Ill: Fermilab. In press
- Wilson, T. L., Rood, R. T. 1979. *Int. Astrophys. Colloq., 22nd, Liège*, p. 503
- Wolff, S. C., Heasley, J. N. 1985. *Ap. J.* 292: In press
- Yahil, A., Beaudet, G. 1976. *Ap. J.* 206:26
- Yang, J., Schramm, D. N., Steigman, G., Rood, R. T. 1979. *Ap. J.* 227:697 (YSSR)
- Yang, J., Turner, M. S., Steigman, G., Schramm, D. N., Olive, K. A. 1984. *Ap. J.* 281:493 (YTSSO)
- York, D. G. 1983. *Ap. J.* 264:172
- York, D. G., Ratcliff, S., Blades, J. C., Cowie, L. L., Morton, D. C., Wu, C. C. 1984. *Ap. J.* 276:92
- York, D. G., Rogerson, J. B. 1976. *Ap. J.* 203:378
- Zappala, R. R. 1972. *Ap. J.* 72:57
- Zwicky, F. 1966. *Ap. J.* 143:192
- Zwicky, F. 1971. *Catalogue of Selected Compact Galaxies and of Post-Eruptive Galaxies*. Guemlingen, Switz: F. Zwicky. 388 pp.